Institut de recherche
en biologie végétale

Université de Montréal

Thèse de Maitrise

Mahsa Naghavi

Studying the cytomechanic aspects of pollen tube growth behavior using Lab-On-Chip technology

Membres du comité conseil:

Mohamed Hijri

Anja Geitmann

Muthukumaran Packirisamy

Printemps 2014

Université de Montréal
Faculté des arts et des sciences
Département de sciences biologique

Table of content

List of figures

memory.

Literature review

1. Plant cell morphogenesis

There are several structural differences between animal and plant cells, one of the most significant being the presence of a polysaccharide wall outside of the plasma membrane of plant cells. Plant development is based on three fundamental processes of cell expansion, cell division and cell differentiation. Since walled cells such as those of plants, algae and fungi do not crawl or migrate; the overall expansion of the cell is the only way for a cell to reach other locations in the organism. Cellular expansion is also fundamental in the generation of the phenotype of the adult plant (Fowler and Quatrano, 1997; Smith and Oppenheimer, 2005; Geitmann and Ortega, 2009). During expansive growth, both the cell size and the shape of the cell change. During differentiation of the cell, the volume of meristem cells increases between 10-1000-fold up to 30 000-fold (in xylem vessels), depending on the type of the cells (Veytsmann and Cosgrove, 1998; Cosgrove, 2005). The expansion is the result of a mechanical procedure that balances the external and internal forces and causes the cell wall to be deformed (Geitmann and Ortega, 2009). It is driven by the hydrostatic pressure called turgor, which is generated through differences in osmotic pressure. Turgor pressure is non-vectorial and hence is applied onto the cell wall equally in all directions (Mathur, 2006; Geitmann and Ortego, 2009). Therefore, cell expansion in cells with uniform and isotropic cell walls will always result in a spherical shape. Any other shapes are generated by modulating cell wall properties to be either non-uniform, anisotropic or both. The regulation of cell wall mechanical properties is therefore crucial for the generation of complex shapes such as those of the jigsaw puzzle shaped cells of the leaf epidermis or the longitudinal shape of shoot and root cells (Mathur, 2006). These cylindrical cell shapes are generated by a largely diffuse growth pattern, as is the case in the roots and shoots (Castle, 1955; Green, 1963; Chen, 1973; Shaw *et al*., 2000). However, in this case

growth has to occur in highly anisotropic manner.

In plant cell morphogenesis, expansive growth is regulated by three important features; (i) the polysaccharidic network forming the cell wall in plants and fungi providing the mechanical structure, (ii) agents modulating the mechanical properties of this network such as newly added polysaccharides, proteins, pH and Ca^{2+}). (iii) the magnitude of the internal hydrostatic pressure caused by turgor (Dumais *et al.,* 2006; Geitmann and Ortega, 2009).

The morphogenesis of plant cells with more complex geometry typically entails the formation of localized outgrowths. These are generated through local modulation of the cell wall properties (Cosgrove, 2000), which in turn is regulated by the underlying cytoskeletal mesh which controls local cell wall assembly (Hepler *et al*., 2001; Mathur, 2004). A spatially confined softer region of the cell wall causes will result in a local swelling which can be the beginning of polar cell expansion and formation of a protuberance (Mathur, 2006). The local cell wall softening and expansion leads morphogenetic processes such as leaf development at the shoot apical meristem and root hair formation from the root epidermis (Hamant *et al*., 2008).

The best examples of local wall expansion are the tip-growing cells, such as fungal hyphae, root hairs, and pollen tubes. In these cells, growth at the tip happens when the material for the cell wall and membrane expansion are secreted and discharged at the very tip or apex of the cells (Fowler and Quatrano, 1997; Bove *et al*., 2008). In plant tip-growing cells that are immobile, morphogenesis and development is regulated at the cortical area. The spatial control of cell expansion and cell division are established in these cortical domains. In plant tip-growing cells, cortical domains are the main keys of directional signals for cell polarity and cell division. Typically, a directional signal helps (causes) the stimulation of an asymmetrical cortex or membrane-associated, called a cortical domain, where the cell wall material is delivered via the cytoskeletal arrays (Fowler and Quatrano, 1997). Therefore, the spatial regulation of plant

cell morphogenesis is mediated by the cytoskeleton, plasma membrane and the secretion of material to the targeted region of cell wall for expansion (Fowler and Quatrano, 1997; Kropf, 1992).

Cell expansion is the result of both the increase in cell size and the change in cell shape (Cosgrove, 2005). In the initiation of polarized growth, actin plays a key role which has clearly been illustrated during rhizoid initiation in spherical fucoid zygotes (Alessa *et al*., 1999), as well as the actin accumulation in tip growing cells (pollen grain germination and root hairs) (Baluska *et al*., 2000; Gu *et al*., 2003), during the initiation of trichomes (leaf hairs) (Mathur *et al*., 1999). Consistent with this notion, the application of an actin inhibitor leads to diffusive and abnormal rhizoid formation in fucus zygotes (Habel *et al*., 2003), inhibition of pollen tube formation in germinated pollen grains (Vidali *et al*., 2001), as well as failing to launch the tip domain in *Arabidopsis* trichoblasts (Baluska *et al*., 2000).

In plant cell morphogenesis, the interaction between the cytoskeleton, plasma membrane and the cell wall was studied to observe cell expansion triggered by directional light in the zygotes of fucoid algae (Kropf, 1992). The signal from the directional light causes an interaction between actin microfilaments and the plasma membrane. This interaction assists in the transmission of a directional trigger in the polar growth reorientation of the cell. This directional signal builds a cortical site for redirection of secretory vesicles from a symmetrical pattern to an asymmetrical distribution (Fowler and Quatrano, 1997).

Studies report that in tip-growing cells of bacteria, budding yeast and animal cells (neurons) the expansion occurs in response to directional triggers of internal or external origins (Horvitz & Herskowitz, 1992; Drubin & Nelson, 1996; Gönczy & Hyman, 1996). In these types of cells, as well, the directional signal requires the asymmetrical exocytosis of material required for cell growth at either a cortex or a membrane. The macromolecules to be targeted (such as proteins) are shipped to the cortex or membrane via a cytoskeletal system. The cytoskeleton has a central

role for controlling both the growth of plant cell and its spatial regulation in directing the cell wall material deposition. In higher plants, as in yeast and *Fucus* (a marine brown algae), the localized cellular expansion could be as follow, firstly by chosen a cortical site, which this site would help to guide the expansion of the neighbouring cell wall. Secondly, the secretion that is necessary for the modification of the wall at this cortical site (Fowler and Quatrano, 1997).

The major structural component in the cell wall that regulates expansion is cellulose, which is synthesized by complexes of enzymes located in plasma membrane. The cellulose microfibril arrangement is important for determining the pattern of cell wall expansion, and it has an important relationship with cortical microtubule organization in growing cells. The arrangement of the microtubules is parallel to the main orientation of the microfibrils, in most plant cells (Pierson *et al*., 1986). The orientation of the cortical microtubules and cellulose microfibrils controls the anisotropic expansion (Wiedemeier *et al*., 2002). When pharmacological agents or mutation disrupts the cortical microtubules, the deposition pattern of cellulose microfibrils is also interrupted. This disrupts the normal deposition pattern, where might cause the breakdown of the tissue boundaries (Wiedemeier *et al*., 2002). The parallel alignment of cellulose causes anisotropic expansion since it reduces expansion in the direction parallel to the fibrils (Green, 1980; Taiz, 1984). Therefore, when cellulose microfibrils are not aligned in parallel any longer, the anisotropic expansion changes to isotropic expansion (Wiedemeier *et al*., 2002).

Unlike cellulose and callose (a related polymer), all other components required for cell wall assembly are delivered to the wall through secretion. These secreted components include a variety of carbohydrates, needed for cross-linking of the cellulose microfibrils; and the enzymes that catalyze both breakage and reforming of cross-links (Schopfer, 2006; Chebli and Geitmann, 2007; Geitmann and Ortega, 2009; Keegstra, 2010). The cytoskeleton is important for cell expansion as it controls secretion in space and time (Smith and Oppenheimer, 2005; Schopfer, 2006; Geitmann and Ortego, 2009; Bove *et al*., 2008).

1.1. Tip Growth

In plant cells, two main types of growth can be distinguished: diffuse and tip growth. In diffuse growth the surface of walled cells expands uniformly over the entire cell surface resulting in a spherical or polyhedral shape (such as potato tuber parenchyma), whereas the growth region of tip growing cells is confined to the extremity of the cell, resulting in a more complex cell shape that in this case is cylindrical. Tip growth is extremely polarized, and the incorporation of new cell wall material as well as the wall expansion is localized. Typical tip-growing cells in plants are pollen tubes and root hairs, and in animals are neurons. The investigation of the mechanical principles governing tip growth has helped us to understand how plant cell morphogenesis functions in general (Mathur, 2006).

In general, plant cell growth relies on interplay between turgor pressure, water absorbance and changes in mechanical properties of the cell wall through modulation of its composition. The turgor pressure applies the necessary force to deform the existing cell wall, which causes the expansion of the cell (Geitmann and Ortega 2009). Simultaneously to wall expansion, new cell wall material needs to be inserted to prevent bursting that would eventually result from the turgor induced stretching of the existing wall. In tip-growing cells the assembly must occur at very fast rates to sustain this rapid process. Cell wall material is quickly transported to and secreted at the tip by secretory vesicles (Bove *et al*., 2008).

As is typical for tip growing cells, the apical cytoplasm of a pollen tube contains a huge number of secretory vesicles (Chebli and Geitmann, 2007; Bove *et al,* 2008). This spatially confined deposition mechanism together with the application of the turgor pressure inside the cell causes the non-uniform mechanical deformation of the cell wall materials, which in turn generates directed cell expansion (Dumais *et al*, 2006). The wall expansion involves simultaneous secretion of new material and wall deformation driven by the turgor pressure (Dumais *et al*., 2006). These two main processes are combined in a model of cell

morphogenesis for tip growing cells (Dumais *et al.* 2006). The turgor driven expansion of the cell wall in tip growing cells is limited to a very small region of the cellular surface, the apex. Since turgor pressure is a scalar factor, this spatial confinement is ensured by a spatial gradient of wall deformability (Chebli and Geitmann, 2007; Fayant *et al.,* 2010). As is the case for diffusely growing cells, tip-growing cells have a stiff wall in the non-growing region to maintain the shape of cell (Cosgrove, 2000) caused by the polar distribution of the cell wall material. The distal deposition of cellulose and callose contribute to the rigidification of the wall, forming the cylindrical shank of the tube. The bulk of the wall material delivered by vesicles is in the form of methyl esterified pectins which, after their exocytosis mature through de-methyl esterification by pectin methylesterase and their subsequent gelation by calcium ions in the shoulders of the apex. This gelation increases the mechanical strength of the pectic material (Geitmann and Steer, 2006, Chebli and Geitmann, 2007). Therefore, the apical cell wall of the pollen tube is rich in methylesterified pectin, while the shank is constructed by two or three cell wall layers of callose, cellulose and de-esterified pectins (Geitmann and Steer, 2006; Aouar *et al*., 2010; Fayant *et al*., 2010). The callose layer is deposited between the plasma membrane and the pectin layer in the distal region of the tube (Parre and Geitmann, 2005). The continuous and highly targeted exocytosis of methyl esterified pectin yields to the turgor pressure (Geitmann and Steer, 2006; Chebli and Geitmann, 2007; Fayant *et al.,* 2010). This gradient of (esterified/de-esteried) pectin in mechanical properties and the spatially controlled process of exocytosis are crucial for morphogenesis of a perfectly cylindrical cell (Fayant *et al*. 2010).

The stiffening in the shank region ensures that the pollen tube expands and elongates only at the tip of the cell (Fayant *et al*., 2010). In walled cells it is possible to stop cell enlargement while wall deposition is maintained for some time leading to local thickening of the cell wall (Roy *et al*., 1999). These authors studied the uncoupling of exocytosis and elongation, via

cytoplasmic calcium concentration and extracellular calcium in *Lilium longliflorum* pollen tubes. The growing pollen tubes were treated with phenylglycoside ($(\beta\text{-D-Glc})_3$), which inhibits growth but not secretion. The arabinogalactan proteins (AGPs) secrete into the tip of pollen tube through Golgi vesicles, the binding of phenylglycoside ($(\beta\text{-D-Glc})_3$) to these proteins blocks the fusion of new cell wall materials. This phenomenon changes the balance of the exocytosis process from the extension growth in the pollen tube (Roy *et al*., 1999). Although the extension of pollen tubes in lily is inhibited, the cell wall components build up, and the exocytosis continues with a disorganized pattern that was suggested to be a result of dynamic changes of calcium ion (Roy *et al*., 1999).

Germination and elongation of pollen *in vitro* requires the presence of calcium in the medium (Bou Daher *et al*., 2009; Brewbaker and Kwack, 1963). The calcium ion is taken up primarily at the apex of the tube, and as a consequence, growing pollen tubes, but not non-growing tubes, display a steep gradient of cytosolic free calcium extending from the apex (high Ca^{2+} concentration) towards the shank (low concentration) (Malhó *et al.,* 1995; Pierson *et al.,* 1994). To investigate the role of calcium, the pollen tubes also were treated with caffeine, a growth inhibitor that reduces the influx of calcium (Ca^{2+}) ion ($[Ca^{2+}]i$). Ca^{2+} is a fundamental element in the growth of pollen tube, and the elongation of a pollen tube depends on cytosolic gradient of $[Ca^{2+}]i$ (Malhó *et al*., 1994; Miller *et al*., 1992; Pierson *et al*., 1994). Roy *et al*. (1999) observed the elongation inhibition of tubes and slight thickening of the cell wall at the apex of tube when they treated the pollen tubes with both substances (caffeine and phenylglycoside). In the treated cells, the calcium gradient of the tip collapses and the calcium influx decreases at the tip, where cell wall thickening occurs (Roy *et al*., 1999). Inversely, if exocytosis is inhibited while turgor is maintained, the wall may rupture (Dumais *et al.* 2006).

Disruption of this cytosolic calcium gradient through BAPTA buffer (1,2-bis(o-aminophenoxy)ethane- N,N,N',N'-**t**etra acetic acid)) and blockage of calcium channels result in

growth inhibition (Pierson *et al.* 1994). In lily pollen tubes, the calcium gradient has been measured to decrease from 3.0 μM at the apex to almost 0.2 μM within the distance of 20 μm. The influx of calcium was measured to be between 1.4-14 pmol/cm^2/s (Pierson *et al.,* 1994). The decrease of the calcium concentration in the shank of the tube has been attributed to the uptake by the endoplasmic reticulum or mitochondria (Pierson *et al.,* 1994; Geitmann and Emons, 2000; Chebli and Geitmann, 2007; Battey and Blackbourn, 1993).

Because of the extremely rapid growth in pollen tubes, all processes involved in regulating it must be precisely regulated and fine-tuned. Turgor needs to be maintained and growth rate regulated, while the delivery of vesicles must be controlled to ensure sufficient pectin molecules are available to sustain expansion (Chebli and Geitmann, 2007, Bove *et al.,* 2008, Fayant *et al*., 2010). Cell wall mechanical resistance controls expansion and therefore the self-similar pattern of shape generation that ensures the geometry of the apex remains constant in time despite its continuous advancement. However, the control of the externally positioned cell wall and its non-uniformly distributed properties eventually lie in the process that is responsible for material delivery. The delivery and targeting of vesicles carrying cell wall material by the actin cytoskeleton has been found to be crucial (Taylor and Hepler, 1997; Geitmann and Emons, 2000; Kovar *et al*., 2000; Vidali *et al*., 2001). Actin filaments have to continuously polymerize in order to keep up with the elongating tip. In addition to delivering vesicles, actin filaments organize the apical cytoplasm (Vidali *et al*., 2001). Remarkably, pharmacological inhibition of actin polymerization inhibits pollen tube growth at drug concentrations that are lower than those required to inhibit long-distance organelle transport (Gibbon *et al*., 1999; Vidali *et al*., 2001; Geitmann and Emons, 2000). These findings indicate that actin dynamics is essential for the process of pollen tube expansive growth. The actin cytoskeleton is a key element linking signal perception pathways and subsequent cellular response. Therefore, there is a potential connection

between cell wall expansion, vesicle trafficking and biochemical pathways of all which are involved in the response triggered by a directional signal.

The cytoskeleton of the pollen tube mainly consists of actin filaments and microtubules. These filamentous proteins are oriented in approximately longitudinal or slightly helical manner relative to the long axis of the cell (Geitmann and Emons, 2000; Chebli and Geitmann, 2007). Both cortical cytoplasm and endoplasm contain actin and transport occurs in opposite directions in these two cellular regions (Geitmann and Emons, 2000; Chebli and Geitmann, 2007). Consistent with the fact that myosin moves only in one direction of the polar actin filaments, the opposite movement directions are caused by opposite arrangement of the actin arrays in the central and cortical cytoplasm (Lenartowska and Michalska, 2008; Kroeger *et al*., 2009). Microtubules are typically located in cortical arrays that are arranged longitudinally (Pierson & Cresti, 1992). In most tip-growing cells, such as pollen tubes and hyphae, nuclear organization, migration and position are controlled by the microtubules (Joos *et al*., 1994; Owens and Morris, 1991; Åström *et al*., 1995; Kaminskyj and Heath, 1996). It was found that microtubule degradation (by oryzalin or colchicine) had no significant effect on the capability of pollen tubes to grow or to invade a mechanical obstacle (Gossot and Geitmann, 2007). However, actin destabilization by latrunculin-B (Lat-B) decreases the ability of pollen tube to invade a stiff medium (Gossot and Geitmann, 2007).

1.2. Directional Polar Growth

To reach their targets, tip-growing cells have to change their direction of growth on their path. Neuron cells need to reach targets that are millimeters or centimeters away through other tissues (Dickson, 2002). Root hairs elongate inside the complex geometry of the soil particles to uptake water and minerals for nourishing the plants (Pei *et al*., 2012). Pollen tubes need to reach the ovary for releasing the sperm cells for fertilization (Taylor and Hepler, 1997; Erbar, 2003;

Shukla *et al*., 1998). This path can be many centimeters long.

Changing the directional growth of the tip-growing cell requires a deviation from the radially symmetrical assembly pattern of the cell wall at the tip (Geitmann and Steer, 2006), which is thought to be achieved by targeting secretory vesicles asymmetrically. The logistics of vesicle transport, mediated by the actin cytoskeleton (Shimmen and Yokota, 2004), a crucial element in the cellular response to an external signal. The role of actin cytoskeleton is fundamental for the turning events in all these tip-growing cells (Mattila and Lappalainen, 2008; Isbister and O'Connor, 2000; Zheng *et al*., 1996; Baluska *et al*., 2000; Cheung and Wu, 2008; Bou Daher and Geitmann, 2011).

Neurons consist of an axon and dendrites to pass chemical or electrical signals through an organism. Axons are able to extend to remote targets by making branches and dendrites are thinner branches that elongate for few hundred micrometres. The signals are transferred to another dendrite or target via synapses. The extension of axons and dendrites occurs at the extremity, the growth cone (Dickson, 2002; Mattila and Lappalainen, 2008). Growth cones can find the correct path toward their targets and they are able to change the direction during elongation. Turning requires the motility of the actin cytoskeleton. There are two groups of actin filaments in the neuronal growth cone: dense parallel bundles of outward oriented filaments (in the plasma membrane of the cell) called filopodia, and a network of loose actin filaments (Dickson, 2002). Filopodia are very important in cell motility in dendritic spines (Dickson, 2002; Mattila and Lappalainen, 2008). During turning, the filopodia extend asymmetrically prior to the growth cone reorientation (Isbister and O'Connor, 2000). In the absence of filopodia, the growth cone is disoriented (Zheng *et al*., 1996).

In plants, root hairs develop in four steps: selections of a bulge site on the surface of the trichoblast, bulge initiation, tip growth of the hair and maturation. The actin cytoskeleton has an important role in all these steps (Pei *et al*., 2012). At the location on the trichoblast surface,

where initiation of the bulge occurs, the actin filaments accumulate and extend extremely toward the bulging apex to form the actin meshwork (Baluska *et al*., 2000). The elongation of root hairs also is limited to the tip, to which secretory vesicles are shipped via the actin cytoskeleton. The role of actin filaments is therefore similar as in pollen tubes (Cheung and Wu, 2008) with an important function in vesicle and organelles movement (Pei *et al*., 2012). Consistent with the inverse fountain streaming pattern, the cytoplasmic structures in the pollen tube appear to be aligned parallel to the long axis of the tube except in the tip region, where they are more randomly distributed (Kroeger *et al*., 2009). Contrary to the high stability of actin in muscle cells (Vartiainen *et al*., 2000; Vartiainen *et al*., 2002), the actin cytoskeleton in rapidly growing plant cell (pollen tubes) is very dynamic.

The organization of the cortical cytoplasm and the regulation of vesicle trafficking in the tip of the pollen tube are controlled by the apical and subapical actin arrays (Kroeger *et al*., 2009) (Figure 1) which continuously polymerizes to keep up with pollen tube elongation. Remarkably, in the pollen tube, only a small portion of the actin is present in filamentous form and a huge pool of polymerizable monomers are available for the continuously ongoing polymerization of the actin array at the growing end of the cell (Staiger *et al*., 2010).

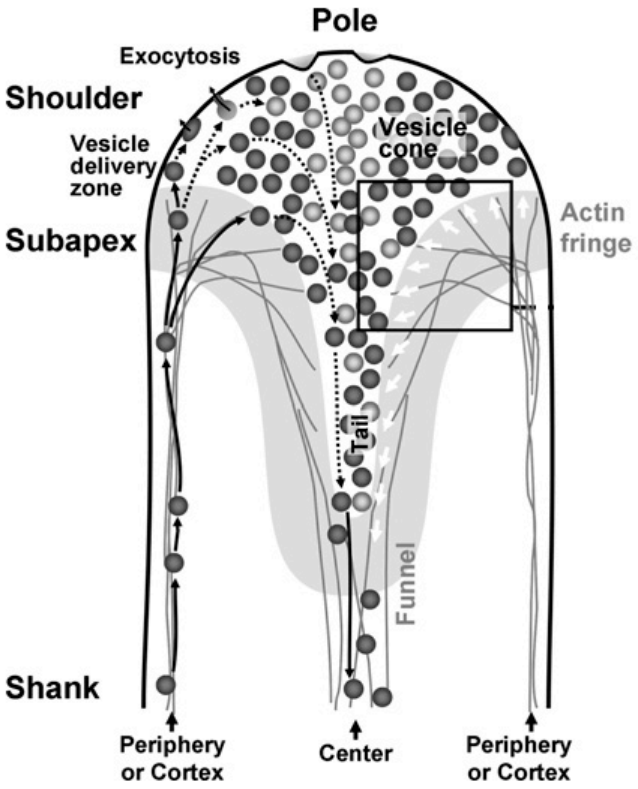

Figure 1. Schematic taken from Kroeger *et al*., (2009) illustrating the directional movement of vesicles and the orientation of the actin filaments in the apical region of a pollen tube. Vesicles are delivered on actin cables and the finer actin filaments of the apical fringe into the apical region, where they are released into the annulus-shaped zone of apical cytoplasm (vesicle delivery zone). Those vesicles that contact the plasma membrane will undergo exocytosis, whereas unsuccessful vesicles will be moved backwards towards the centre of the cone-shaped vesicle pool. Solid arrows represent the movement of actin-myosin-guided vesicles, and dashed arrows represent those movements most probably governed by diffusion. This schematic is not drawn to scale and no other organelle or the cell wall is shown.

The vesicle transfer and movement in the pollen tube from the Golgi bodies to the tip is a myosin-mediated process that requires energy in form of ATP (Bove, *et al*., 2008; Shimmen and Yokota, 2004), whereas microtubules are not required for organelle transport in the pollen tube (Åström *et al*., 1995).

The activity of calcium channels, actin dynamics and the concentration of cytosolic calcium are symmetrically distributed around the central axis going through the pole of the tube, in a growing pollen tube (Bou Daher and Geitmann 2011, Malhó *et al.,* 1992). Bou Daher and Geitmann (2011) analysed the temporal sequence of events leading up to a change in growth direction, using a galvanochamber setup. Both the vesicle pool and actin fringe were found to tilt prior to a visible change in growth geometry suggesting the actin polymerization occurs at different speeds in the two sides of the pollen tube. Actin polymerization seemed either to be slowed down in the cathodal side or enhanced in the anodal side to allow the tube to bend

towards the cathode (Bou Daher and Geitmann 2011). This asymmetric growth activity is likely regulated by actin binding proteins, for example ADF7 and ADF10 (Bou Daher *et al*., 2011).

2.1. Cytoarchitecture of the pollen grain

Pollen grains vary in size (from 10 to 100 μm); shape (round, oval, disc, bean-shaped and filamentous); color (ranging from white, cream, yellow or orange to green and blue); surface structure of the cell wall (from smooth to spiky) and the number and position of germinating apertures (Wodehouse, 1928; Sporne, 1972; Hill and Lord, 1987; Moore *et al*., 1991). In angiosperms (flowering plants), the mature pollen grain is comprised of two or three cells, depending on the species. Most of the volume of the grain is occupied by the vegetative cell and surrounded by its cytoplasm is either a generative cell (two-celled pollen) or two sperm cells (three-celled pollen). In two-celled pollen the generative cell will divide into two sperm cells during pollen tube growth. The pollen grain is the result of meiosis followed by several mitotic cell divisions and all cells are therefore haploid (Edlund *et al.*, 2004; Yang and Sundaresan, 2000).

The pollen grain is surrounded by a wall that in the mature pollen grain consists of three principal strata (layers) (Figure 2). 1) The external layer is comprised of several ingredients including lipids, pigments, proteins and scented complexes, which cover the holes on the pollen grain exine. 2) The outer wall (exine) is thick, rigid, multilayered and composed of the chemically a resistant polymer, sporopollenin. This layer is interrupted at the germination pores, the apertures. The thick outer layer of the exine lies over the inner layer that extends around whole pollen grain surface and is cutinized all over the pores. The outer exine layer consists mainly of stable biopolymers containing fatty acids. The inner layer of the exine is composed of callose, cellulose and hemicelluloses. The inner layer is cutinized, relatively thick, and uniformly structured except for the germinal aperture where it is broken into granules or

platelets. These layers protect the vegetative and generative cell against mechanical and chemical damage, as well as from environmental conditions such as ultraviolet radiation of the sun. 3) The inner wall of pollen grain (intine) is sometimes multilayered and consists mainly of cellulose. It can be of varying thickness, depending on the species, and it typically is much thicker in the apertural region. Although a thin layer of pectin covers most of the pollen grain surface, around the aperture region a thicker layer of pectin exists. The pectic layer is important during pollen grain hydration since it aids with water absorption. The resulting swelling of the grain can fracture the exine at the aperture during the initial phase of germination (Edlund *et al.*, 2004; Zinkl *et al.*, 1999; Nakamura and Miki-Hirosige, 1985; Ehrlich, 1959; Wodehouse, 1928).

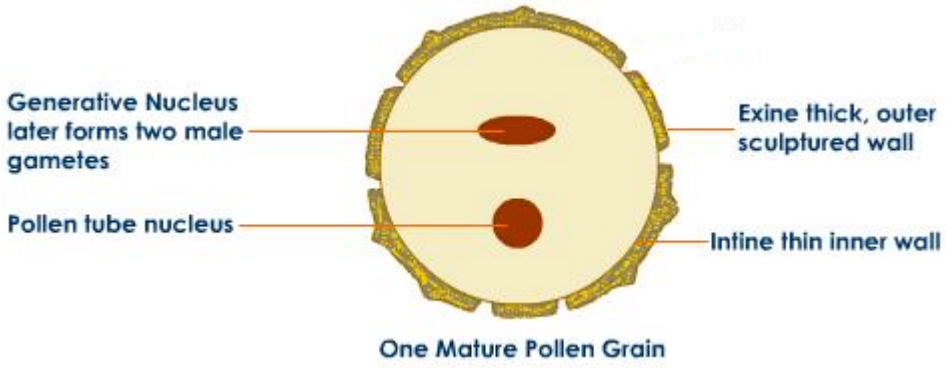

Figure 2. Schematic presentation of pollen grain wall. The thick exine forms the outer wall of pollen grain. A thin layer of intine is located beneath the exine. (http://www.tutorvista.com/content/biology/biology-iv/flowering-plants-reproduction/sexual-reproduction.php)

2.2. The pollen tube

The pollen tube delivers the male gametes into the ovule to reach the female gametophyte. Successful growth and tube elongation, therefore, provides a fundamental link between fertilization and seed setting during reproduction. The distance between the stigma and ovule varies depending on the species and can be tens of centimeters (Figure 3 and 4) (Erbar, 2003). Given that the speed of pollen tube growth counts as a competitive factor, which directly affects the probability of successful fertilization, the growth rates of pollen tube are rather impressive and range up to 1 cm/h (Bou Daher, 2011; Taylor and Hepler, 1997).

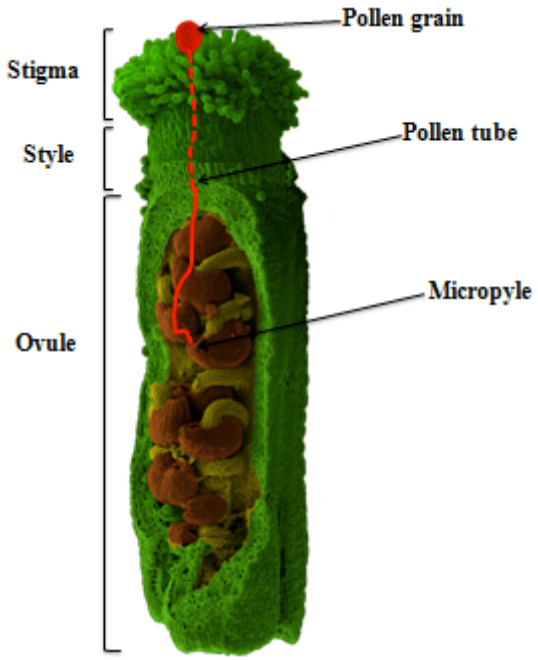

Figure 3. Scanning electron micrograph of *Arabidopsis thaliana* pistil with false colors (Bou Daher, 2011). The schematic representation of the pollen tube (red) shows the pathway of pollen tube through style to reach the micropyle of ovule.

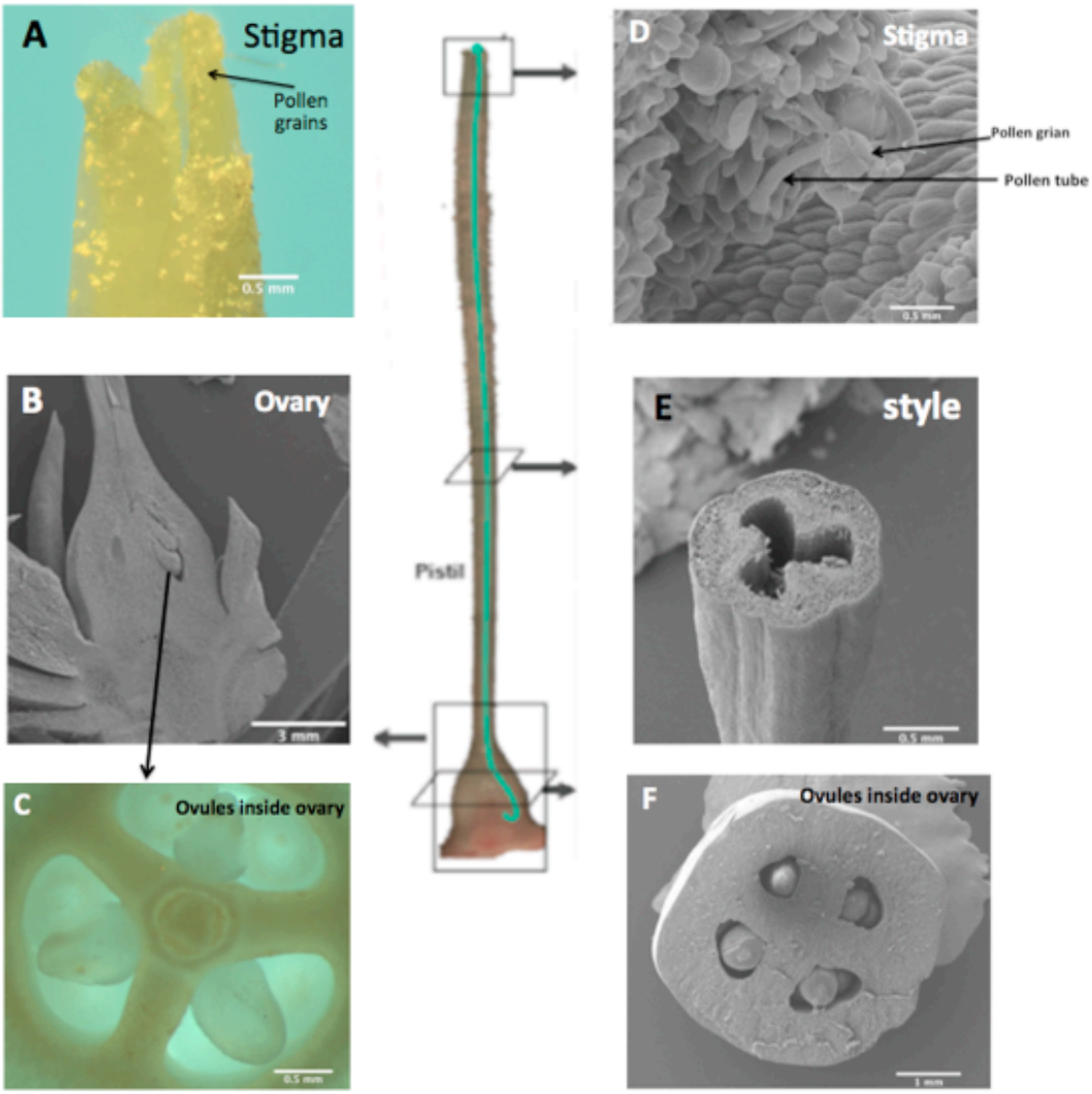

Figure. 4. The pistil of *Camellia* and the pollen tube passageway through the pistil from stigma to ovule. The length of *Camellia* pistil is about ~30 mm (image taken by stereomicroscopy of live samples (color images). The elongating pollen tube (green tube) has to enter and penetrate the style toward the ovary. The *Camellia* pistil has a hollow style (E, scanning electron micrograph of fixed samples (gray scale)) that does not represent a mechanical obstacle. At the transition between style and ovary, the elongating pollen tube reaches mechanical barriers such as the micropyle opening of the ovule, the nucellus, and the filiform apparatus of the synergids. Scale bars: A, C, E, D = 0.5mm. B=3mm. F=1mm.

Pollen tubes are formed following rehydration from the pollen grain by emerging from the aperture. Pollen tube expansion occurs at a very small region of apex to reduce the friction with the tissue through which it passes during its invasive growth (Sanati Nezhad and Geitmann, 2013).

Consistent with polarized growth of the pollen tube, the cytoplasm displays distinct zones: the apical growth zone, the smooth ER (endoplasmic reticulum) zone, the rough ER zone, the vacuolation zone, and the deterioration zone (Uwate and Lin, 1980; Mascarenhas, 1993; Malho, 2006). The cytoplasm of a pollen tube in growing tip region contains a huge number of secretory vesicles and no larger organelles are usually present. Most of the other organelles (mitochondria, dictyosomes and ER) are located in the subapical (non-growing) and distal regions moving along the longitudinal axis of the cell at the rate of micrometers per second (Chebli and Geitmann, 2007; Bove *et al,* 2008). Each minute, tens of thousands of vesicles deliver their material and components required for cell elongation to the apical pool of secretory vesicles. It has been calculated that for a lily pollen tube growing at 7 μm/min, approximately 24,000 vesicles per minute are required to deliver the necessary cell wall material to the apical region (Bove *et al*., 2008). The location of the apical vesicle pool also corresponds to the proximal end of actin fringe, which represents the scaffold along which all organelles are transported (Bove *et al.,* 2008).

As it is shown on Figure 5, the arrangement of endomembrane, mitochondria, vesicles, and other organelles seem to follow the cytoplasmic streaming pattern that, in angiosperm pollen is organized in the shape of an inverse fountain (Mascarenhas, 1993; Malho, 2006).

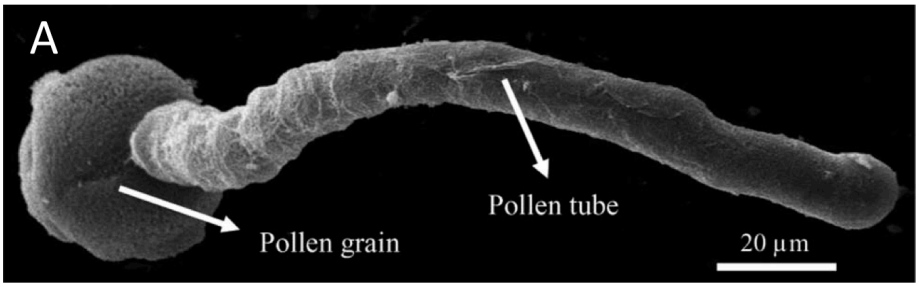

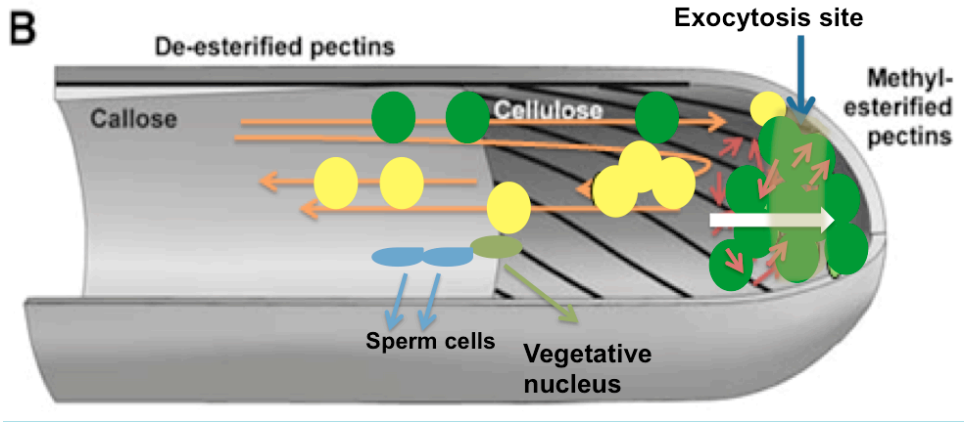

Figure 5. Cellular structure of the pollen tube. A) Scanning electron micrograph of *Camellia japonica* pollen tube germinated in vitro. Scale bar = 20 µm). B) Schematic representation of the pollen tube cytoarchitecture and polar cellular structure; apical cell wall of the pollen tube contains pectin polymers (methylesterified pectin) and the shank is composed of two or three cell wall layers comprising mainly callose, cellulose and de-esterified pectins (Aouar et al., 2010). When pectin methyl esterase is secreted at the apex of the tube via vesicle exocytosis, methylesterified pectin becomes de-esterified (Geitmann and Steer, 2006). Orange arrows represent cytoplasmic streaming parallel to the longitudinal axis, forward movement in the cortex and rearward in the centre of pollen tube. The red arrows represent vesicle trafficking and movement of secretory vesicles (green spheres) accumulating in the apical region shows the exocytosis process and endocytosis (yellow vesicles) taking place at the base of apex. The white arrow represents growth direction of pollen tube to the axis length in normal cells. Objects are not drawn to scale.

3. Sexual plant reproduction

On the way to the female gametophyte, the male gametophyte enters into contact with numerous tissues of the sporophyte (Figure 1). The pollen grain adheres to the stigmatic papilla. During elongation the tube comes into contact with the stylar transmitting tissue and the placenta cells of the ovary (Geitmann and Palanivelu, 2007; Lord and Russell, 2002; Cheung and Wu, 2001; Esau, 1977). Because of the complexity of the path through which the pollen tube has to grow, it needs to follow the guidance cues provided by the pistillar tissues and the female gametophyte. These cues are both of mechanical and chemical nature. The ability of the pollen tube to turn in response to chemical triggers emitted by the female gametophyte has been demonstrated using the *in-vitro* system of *Torenia* (Higashiyama and Hamamura, 2008). *In vitro* growing pollen tubes were exposed to isolated ovules and even when these were relocated, the tubes followed. The precise target area for tubes grown in this setup was the micropylar end of the protruding embryo sac (Yetisen *et al.,* 2011; Higashiyama and Hamamura, 2008; Geitmann and Palanivelu, 2007; Palanivelu and Preuss, 2000; Hülskamp et al., 1995). These *in vitro* experiments are relevant, since *in vivo*, the tube repeatedly has to change its growth direction to find its target. Pollen tube growth is therefore an effective model system to study tropic growth behaviour at the cellular level. Numerous studies have attempted to identify the nature of the signalling agents emitted by the pistil and female gametophyte, such as sterols and lipids (Major *et al*., 2009; Chantha *et al.*, 2007; Germain *et al*., 2006). Recently peptides, azadecalin-like molecules produced by *Arabidopsis* pistils that promote rapid fertilization by suitable pollen and germination (Qin *et al.*, 2011), but the behaviour of the pollen tube proper upon perception of these signals is poorly characterized.

The pollen tube elongates inside the pistil at rates that vary between micrometers/hour to centimeters/hour. The *in-vitro* growth of pollen tubes from commonly used species shows

different growth rate in *Arabidopsis* (13.20 μm/h) (Gebert *et al.,* 2008)*, Camellia* (1-2 mm/h) (data from our lab)*, Nicotiana tabacum* (1.7 mm/h) (Sanchez *et al*., 2004), *Colchicum autumnale* (2.75 cm/h) and maize (1 cm/h), (Sanati Nezhad *et al.,* 2013a and d; Taylor and Hepler, 1997). In *Lilium longiflorum*, the growth rate varies between 2 mm/h (*in vivo*) (van der Woude and Morré, 1968) and 0.5 mm/h (*in vitro*) (Bou Daher *et al*. 2011). The range of growth rates of taxa in ancient angiosperms (*Amborella*, *Nuphar*, and *Austrobaileya*) is 80 to 600 μm/h. The growth rate of pollen tube in gymnosperms is generally <20 μm/h. The calculated maximum growth rates for gymnosperms *in vivo* are ≈1μm/h in *Zamia* (Cycadales), 2 μm/h in *Ginkgo* (Ginkgoales), 5 μm/h in *Gnetum* (Gnetales), and 6 μm/h in *Agathis* (Coniferales). *In vitro* growth rates of other various gymnosperms, however, are in the same range of <1 μm/h in *Pinus* to 10–20 μm/h in various other gymnosperms (Williams, 2008).

The cellular mass of transmitting tissue represents the pathway for pollen tube, after the pollen grain lands on the stigma and germinates. After penetration inside the transmitting tissue, the tube reaches the ovary and passes to the internal surface of placenta (Erbar, 2003). The signals emitted from the female gametophyte guide the pollen tube toward the funiculus, where the ovule attaches to the placenta. Then the pollen tube targets the micropyle, the aperture of the shell that covers the ovule. The pollen tube then has to pass another gate in order to reach the female gametes. Invading the micropyle allows the pollen tube to cross the tissue layer called nucelleus that covers the female gametophyte. After invading, the pollen tube will meet the synergid cells adjacent to the egg cell. When the tube penetrates the filiform apparatus of one synergid, it bursts to release two sperm cells. One fertilizes the egg cell to generate a zygote that will develop into the embryo, and the other combines with the central cell to give rise to the endosperm that is responsible for nourishing the embryo (Taylor and Hepler, 1997).

4. Invasive growth

Tip-growing cells typically have to invade and penetrate the surrounding area to reach their destination. Root hairs extend through the soil to uptake water and mineral nutrients to feed the plant. Fungal hyphae either absorb the nutrients from a biotic host or penetrate abiotic substrate in search for nutrients and water (Takemot *et al*., 2006; Harris, 2008; Haling *et al.,* 2013). In our model system, the pollen tube is challenged by different cell structures from the dry or glandular stigma toward the stylar transmitting tissue and the placenta tissue of the ovary and finally the surface of the funiculus and ovule (Cheung and Wu, 2001; Esau, 1977) (Figure 3 and 4). The pollen tube therefore encounters a series of mechanical obstacles while it attempts to reach its target and accomplish its tasks.

The type of style that pollen tube passes through to reach the ovary could be either hollow or solid depending on the species. In the case of solid style pollen tube needs to invade the apoplast of the transmitting tissue. The transmitting tissue contains an intercellular matrix containing ingredients required for pollen tube growth such as sugars, glycoproteins, and amino acids (Cheung and Wu, 2001; Lord, 2003; Geitmann and Palanivelu, 2007). During the passage of the pollen tube via the transmitting tissue matrix, it has to push and overcome the mechanical obstacle represented by the apoplast. The secretion of digestive enzymes such as hydrolytic enzymes, glycosidases, and the wall loosening protein expansin, by the pollen tube can assist its penetration (Graaf and Derksen, 2001; Cosgrove, 2000).

To transfer the sperm cells safely to the ovary, especially in the case of a solid style, the pollen tube has to withstand the lateral pressure exerted by the transmitting tissue and keep its tubular shape to enable the sperm cells to continue moving forward within the tube. The ability to invade a matrix and avoid collapse makes tip-growing cells interesting objects to study invasive growth. Understanding the mechanical aspects of invasion helps us to understand the biological principles governing the functioning of these cells.

From earlier experiments we know that the pollen tube's ability to penetrate a stiffened matrix is affected upon pharmacological manipulation of the cytoskeleton (Gossot and Geitmann, 2007). However, this test was done using agarose, the mechanical properties of which are not calibrated. Here we wanted to use an *in vitro* system that imitates the *in vivo* conditions better and in more calibrated manner of mechanical forces.

Measuring the invasive force of the pollen tube is technically challenging. The invasive force of fungal hyphae, however, was measured using a miniature strain gauge (Money, 2004), but the huge size of cantilever (100µm thickness and 10 mm width compared to the size of the cell 10µm) was its greatest disadvantage as imaging is challenging. In a different approach the invasive force of infection hyphae was measured using a synthetic membrane as a waveguide (Bechinger *et al*., 1999). However, this requires the adhesion of an appressorium to the membrane and can thus not be used for pollen tubes. To measure the forces exerted by growing pollen tubes we developed an experimental set-up using Lab-On-Chip (LOC) technology.

5. Objectives

The principal goal of my project is to characterize the mechanisms that enable the pollen tube to navigate the mechanical obstacles presented by the pistillar tissues and to respond to directional triggers. The following are the detailed objectives:

1. Developing the Lab-On-Chip platform to study the mechanical aspects of individual pollen tubes.
2. Studying the invasive growth of pollen tubes using the Lab-on-Chip platform

   2.1. Quantifying the dilating force of pollen tubes to invade narrow spaces

   2.2. Studying the ability of pollen tubes to navigate mechanical obstacles

3. Assessing the suitability of the Lab-On-Chip platform for high-resolution and fluorescence microscopy.

Chapter 1. Development of the microfluidic platform TipChip

This chapter explains our collaboration with the laboratory of Professor Packirisamy at the Mechanical and Industrial Engineering Department, Concordia University. Three graduate students (A. Sanati Nezhad, M. Ghanbari, and C. Agudelo) of the Packirisamy lab fabricated the TipChip devices using soft lithography techniques. I performed experimental tests in collaboration with the Packirisamy lab members. The data were published in four papers (Agudelo *et al*., 2012, 2013a and b; Sanati Nezhad *et al*, 2013a, b and d). The present chapter focuses on the aspects in which I was directly involved. I contributed Figures 7i, 8c, 8d in this chapter while the other figures were prepared by the co-authors.

Summary

Studying the mechanical aspects of plant tip-growing cells *in-vitro* is challenging since the size of the measuring device needs to be in the same dimension as that of the cell. To be able to simulate the growth conditions that a pollen tube encounters in the *in vivo* situation, in collaboration with the laboratory of Dr. Packirisamy, Concordia University, we developed a series of microchips that mimic mechanical obstacles and serve to measure the biomechanical properties of growing pollen tubes. We developed TipChip microfluidic devices system based on Lab-On-Chip technology. These microfluidic devices are made from PDMS (polydimethylesiloxane) with soft-lithography. Our developed TipChip micro devices allowed us to study the growth behaviour and mechanical features of pollen tubes. To ensure reproducible growth conditions we studied the effects of varying the growth medium flow rate, the depth and the width of microchannels on the growth velocity of pollen tubes. Through our collaboration, the LOC devices considering the basic design of channels were fabricated and

tested for fluid flow rate. I contributed to several of the experimental assays and I tested the compatibility of LOC devices with fluorescence microcopy.

1.1. Introduction

The walled cells of plants have a stiff extracellular matrix outside of the plasma membrane that influences growth, division and differentiation of the cells. The polarized growth of certain walled cells is therefore an interesting phenomenon, since in addition to growing in size, the cell actually exerts forces against the surrounding substrate. Well investigated tip-growing cells include root hairs, fungal hyphae and pollen tubes (Money, 2004; Brand and Gow, 2008; Palanivelu and Johnson, 2011; Winship *et al*., 2011).

Growth and morphogenesis of walled cells are a result of cellular expansion involving the deformation of the cell wall driven by water uptake. In pollen tubes, the cellular expansion occurs at the very end of the cell and at the same location new cell wall material is assembled resulting in a cylindrical protuberance with oval or hemispherical shaped apex. The delivery of new cell wall material and the turgor pressure applying stress on the cell wall are necessary to generate the actual growth process (Rojas *et al*., 2011; Geitmann and Ortega, 2009; Geitmann and Dumais, 2009; Geitmann and Steer, 2006; Harold *et al*., 1995).

Besides growing rapidly (up to 1 cm/h in pollen tubes and fungal hyphae), tip growing cells are able to control the direction of growth, a skill that they share for example with neurons (Palanivelu and Preuss, 2000). To answer many of the open questions regarding these cell types, we need to develop methods that enable us to carry out more complex experiments, as well as large-scale phenotyping. Here I describe the microfluidic platform developed in collaboration with our colleagues at Concordia University with the aim to investigate single tip growing cells in highly reproducible manner. This TipChip platform has been tested and optimized for pollen, but it could easily be used for other tip-growing cells such as hyphae (fungal) and moss

protonemata (moss spores).

Since the pollen grains are easy to collect, store, and germinate, we chose the pollen tube as a model system to optimize our technology of Lab-On-Chip (LOC) and study the mechanical behaviour of tip-growing cells. This technology allows the construction of miniature devices that can be designed to simulate certain properties of the tissues through which pollen tubes have to grow in the plant. Yetisen *et al* (2011) were the first to use such a micro-device in order to analyze the behaviour of pollen tube in response to isolated ovules. However, their micro-device design is very simple, consisting of a main central groove and side chambers in one of which the ovules were placed (Figure 6) and the dimensions of the structures are orders of magnitudes bigger than the cells.

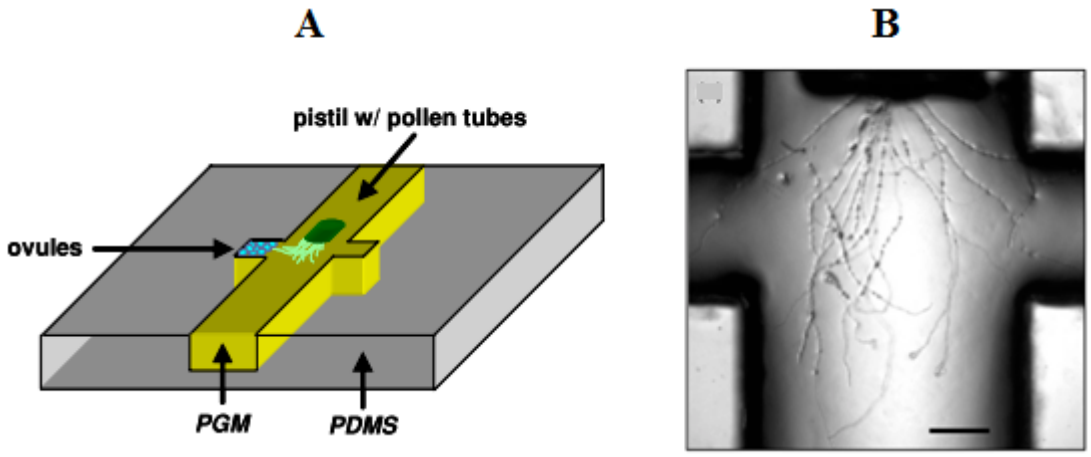

Figure 6. Micro-device for growing pollen tube. (A) Schematic of micro-device showing the overall setup of the system. (B) Close-up of grown pollen tubes inside the system. Provided by Yetisen *et al.,* (2011). Scale bar =200µm.

The dynamic regulation of tip growth via temporal and spatial control has been studied in different laboratories (Feijó *et al*., 2001; Hepler et al., 2001; Money, 2001; Money et al., 2004;

Malho, 2006; Cheung and Wu, 2007, 2008; Geitmann and Palanivelu, 2007; Brand and Gow, 2008; Palanivelu and Tsukamoto, 2011; Qin and Yang, 2011). In the past, pollen tube performance has typically been assessed based on quantification of seed set (*in vivo*), quantification of germination percentage (*in vitro*), average growth rate (*in vivo* and *in vitro*), and on cell morphology (*in vitro*). While these approaches provide excellent quantitative information using bulk samples (e.g. Bou Daher *et al.* 2008) more detailed information can be gained from more specific approaches. Among these are the vibrating probe, a technique that allows monitoring ion fluxes (Feijò et al., 1995; Messerli and Robinson, 1997, 1998, 2003), a microindenter to measure the biomechanical properties of pollen tubes (Geitmann et al., 2004; Parre and Geitmann, 2005a,b; Zerzour et al., 2009), and microstructured obstacles and directional triggers to investigate invasive and tropic growth (Malhò et al., 1992; Palanivelu and Preuss, 2000; Lord, 2003; Gossot and Geitmann, 2007; Higashiyama and Hamamura, 2008; Amien *et al*., 2010; Bou Daher and Geitmann, 2011; Palanivelu and Tsukamoto, 2011).

A miniature strain gauge has successfully been used to measure the invasive force of fungal hyphae (Money, 2004). The size of the silicon beam used (a cantilever of 100 μm thickness and 10 mm width) compared to the size of the cell (10 μm) is the disadvantage of this method as it renders precise imaging of the process difficult and the silicon beam is not soft enough to sense the cellular force with sufficient precision. In addition, the parameters such as the shape of cell, growth inhibition, or a shift in growth direction cause the data to be rather variable. Money (2004) also measured the hyphal force using an indentation technique based on a synthetic membrane used as a `waveguide` (Bechinger *et al*., 1999). This method requires the fungal appressorium to adhere to the membrane. Germlings of pathogens typically secrete an adhesive along the elongating germ hypha that allows them to attach to the surface (Money (2004). *In vivo* grown pollen tube of lily are also known to produce clusters of F-actin as a sort of internal structure that might connect to external attachments (Pierson *et al*, 1986), when the tube passes

through the pistil from stigma to ovary. However, this configuration and adhesion was not detected *in vitro* (Park *et al*., 2000). Pollen grains or tubes do not adhere to artifical membranes and hence this method would not work.

These techniques, although useful, are time-consuming, since only one cell can be tested at a time and results are highly variable. Our newly designed platform allows us to examine several tip-growing cells at the same time, and in highly reproducible manner. Since the platform's design is flexible, it makes an ideal system for both phenotyping and developing new experimental methodologies for the investigation of tip-growing cells.

The TipChip platform is based on microelectromechanical systems (MEMS) technology. This technology has been exploited in biological and medical applications to simplify sophisticated functions such as chemical reactions, drug development and bioassays by integrating them within a single micro-device, called a Lab-on-a-Chip (LOC; Cheung and Renaud, 2006; Giouroudi et al., 2008; Nuxoll and Siegel, 2009).

In this chapter I briefly describe the geometry and fluid flow conditions of the LOC as developed and optimized by our collaborators in the Packirisamy lab (A. Sanati Nezhad, M. Ghanbari, and C. Agudelo). The versatility of the device is illustrated by several experimental assays. This work has been published (Sanati Nezhad, *et al*., 2013a, b, c and d, and Agudelo, *et al*., 2013, 2014). I was involved in testing most of these devices and I performed my experiments using bright field and confocal laser scanning microscopy (Figures, 7i, 8c, and d,).

1.1.1. Microfluidic devices imitating *in-vivo* conditions

In nature, the pollen grain on the stigma germinates after hydration and then the pollen tube grows through the stylar tissue to reach to the ovary (Lord and Russell, 2002). On this path, the pollen tube faces different structures from the dry or glandular stigma, the stylar transmitting tissue, the placenta tissue of the ovary and finally the surface of the funiculus and ovule (Cheung and Wu, 2001; Esau, 1977) (Figure 3). The ability to invade the apoplast of the transmitting tissue is a requirement for successful pollen tube growth, since the appoplast acts as a mechanical obstacle for passing pollen tube. Furthermore, the tube has to resist any lateral pressure exerted by the transmitting tissue to keep its tubular shape and permit the passage of the sperm cells. The purpose of the microfluidic device was to mimic this situation in the transmitting tissue in order to understand the mechanism that allows the pollen tube to exert its delivery function against the impedance of the pistillar structures. We achieved this by a variety of design features. An overview of the designs and fabrication methods is represented in section 1.3. Agudelo *et al*. (2012) described in detail the fabrication of the LOC devices.

1.1.2. Design and Fabrication

The TipChips were fabricated using soft lithography technique (Agudelo *et al*., 2012). This entails the production of a photomask that is used to project a pattern onto the photoresist. Tests done by Agudelo *et al* (2013) for photomask production methods (digital printing at 3600 dpi and direct writing laser (DWL) lithography), revealed that using the DWL lithography technique the surface of microchannels are smoother. This more precise technique is expensive, but is necessary to ensure that the microstructured features have a resolution that is precise enough for the dimensions of pollen tube (see Figure 8 for examples of both techniques).

The microfluidic networks are made from polydimethylsiloxane (PDMS) using a silicon/SU-8

mold and the microfluidic designs are adapted to meet the criteria of individual experimental approaches. The PDMS at the entrance and exits of the microfluidic network was punched to make an inlet and outlets. The final fabricated microfluidic network of PDMS was sealed by a cover slip (Squares No. 2; Thickness: 0.17 to 0.25mm; Size: 25mm, http://www.fishersci.com; Harrick Plasma PDC-001, http://www.harrickplasma.com) to make the devices compatible for microscopy using high numerical aperture objectives. Plastic tubes were inserted at the inlet and outlets. The pollen grain suspension and growth medium was injected into the device via the inlet, and the circulation through the microfluidic network and

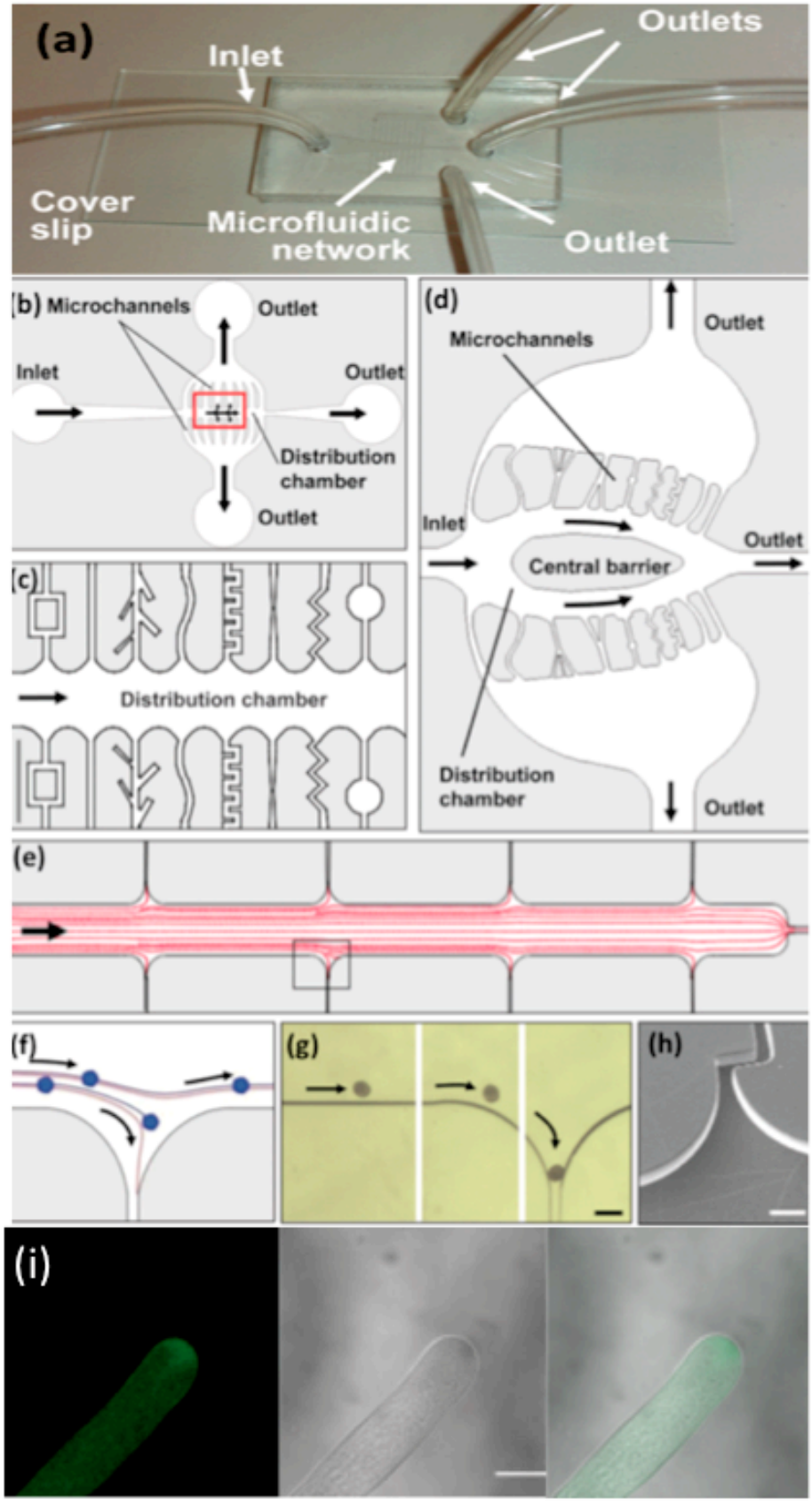
(a)
Inlet
Outlets
Cover slip
Microfluidic network
Outlet
(b) Microchannels
Outlet
Inlet
Outlet
Distribution chamber
Outlet
(c)
Distribution chamber
(d)
Microchannels
Outlet
Inlet
Central barrier
Outlet
Distribution chamber
Outlet
(e)
(f)
(g)
(h)
(i)

Figure 7. Basic design of the multichannel TipChip platform.

(a) Image of the TipChip showing the PDMS layer attached to a cover slip, with inlet and outlets. (b) Design of the microfluidic network in the TipChip. The pollen suspension is injected via the inlet; laminar flow moves the pollen grains through the distribution chamber, where the grains are trapped at the entrances of the microchannels. Excess fluid and pollen grains are evacuated through the distribution chamber outlet. (c) Rectangular portion of distribution chamber of the TipChip as shown in (b), illustrating various types of microchannel geometries. Scale bar = 500 µm (dark gray in lower left corner). (d) Alternative design with central barrier. (e) Fluid flow streamlines within the distribution chamber. (f) Detail of image (e) providing the simulated streamlines detail (red) with the movement of experimentally observed pollen grain (blue) through the distribution chamber. (g) Micrographs of trapping a pollen grain at the microchannel entrance. A single pollen grain is shown at three different times as it is driven by fluid flow indicated by the arrow. Scale bar = 100µm. (h) Scanning electron micrograph of a trap entrance. Scale bar = 100 µm, from Agudelo *et al*., (2013); (i) Pollen tube growing in an LOC and labeled with FM1-43 to reveal vesicles is shown in fluorescent mode (left), in brightfield mode (middle) and in an overlay of both (right). Scale bar = 20 µm.

the exit of the growth medium was controlled at the outlets.

For simultaneous observation of multiple cells, the set-up needed to contain multiple microchannels. Ungerminated pollen grains in growth medium solution are injected and only upon placement the pollen grains germinate to form the tubes. Using laminar fluid flow, the pollen grains are guided toward the microchannel entrances where they are trapped. The main platform of microfluidic network contains an inlet, a distribution chamber with access to eight microchannel entrances, and two different kinds of outlets - one for the evacuation of excess pollen grains from the chamber and others to drain liquid from the ends of the microchannels to allow a continuous flow of liquid. The enclosed microchannels prevent evaporation of the growth medium surrounding the cells. Evaporation is a technical problem in open microchannel systems (Yetisen *et al*. 2011).

The height of the distribution chamber was normally between 1.2 and 1.5 times the pollen grain diameter to avoid the accumulation of the grains inside the chamber, which would create a mechanical barrier for the fluid as well as preventing microscopical observation. The pollen grain of the species used in this study, *Camellia japonica*, is 60 μm wide. Therefore, the height of the microfluidic network was set to 80 μm. The width of pollen tube of this species is 14 to 20 μm and it has a very fast and straight growth. These characteristics of *Camellia japonica* make it a perfect model system for cytomechanical research as established previously (Bou Daher and Geitmann, 2011). However, while the current version of the TipChip is optimized for *Camellia*, it can easily be adapted for the use with either pollen from other species or fungal spores.

The design of the microfluidic network had to provide for the particular challenges associated with our cellular system. We wanted to trap pollen grains and immobilize them in the presence of continuous fluid flow and the emerging pollen tubes were supposed to grow into narrow microchannels in which experimental design features could be incorporated. Earlier

devices (Tan and Takeuchi, 2007; Kobel *et al*. 2010) trap a relatively small number of particles in short microchannels. In contrast we wanted to trap individual pollen grains at one end of long channels, and to observe many growing pollen tubes in the device. Also, we wanted to ensure that only one or few pollen grains would be trapped at each microchannel entrance, since accumulations of pollen grains would build a mechanical barrier for the circulation of fluid flow potentially affecting the experimental conditions and the reproducibility of the experiments.

Two different geometries were tested for the distribution chamber (Agudelo *et al*., 2013): a simple rectangular shape (Figure 7b, c) and an oval shape containing a central barrier (Figure 7d). Pollen grains were trapped at entrances through transportation of laminar fluid flow created by slow injection of pollen suspension (Sanati Nezhad *et al*., 2013d). To trap the grains at the entrance, the end of the mirochannel was designed as a curved notch, smaller than the size of pollen grains (30 μm). The pollen tubes are then guided through the narrow canals of the microchannels. Depending on the desired experimental conditions, the microchannels could be equipped with mechanical obstacles, chemical gradients, electric fields, and biosensors (Figure 7c) (Agudelo *et al*., 2013).

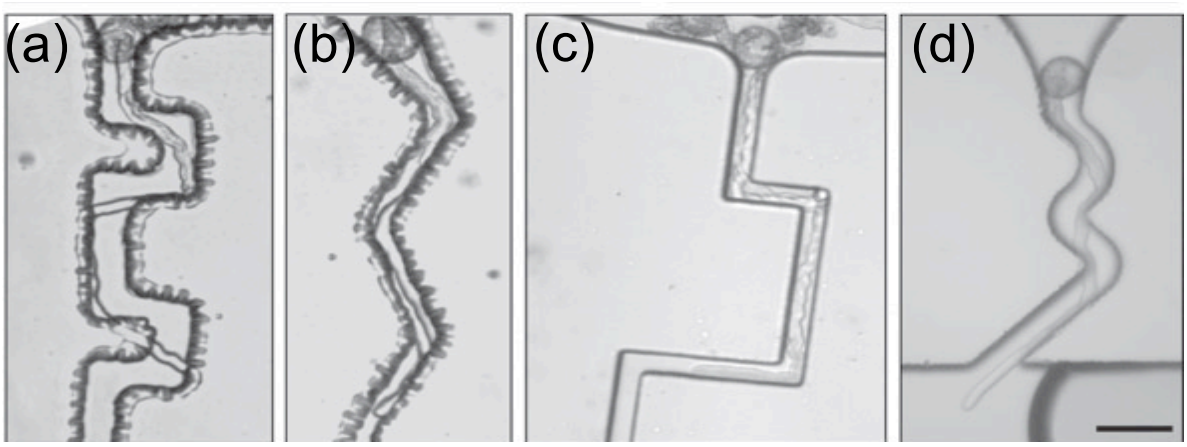

Figure 8. Microchannel fabrication using two high-resolution methods. (a, b) The fabrication of microchannels provided by a transparency film photomask, which is taken by high-resolution digital printing (3600 dpi). (c, d) Microchannels is fabricated using a high-resolution glass mask created by direct-write lithography. The smooth surface of PDMS in (c) and (d) is the reason for choosing this higher-resolution technique in the microchannel fabrication. Scale bars = 100 lm. Image is from Agudelo *et al* (2013).

1.2. Design and fabrication of LOC platform

The design of the channels has to take into consideration the size of the pollen grain and the pollen tubes of the species to be used. The selected species for this study is *Camellia japonica.* The pollen grains germinate very quickly (20 to 30 minutes after imbibition) and the tubes grow very fast (0.2 μm/sec) thus minimizing experiment timeAlso, compared to other species (such as *Arabidopsis*), the tubes have a large diameter (approximately 18 μm), making *Camellia* an excellent model species to study the mechanical properties of the pollen tube. This species will be used for those portions of the project that pertain to cell mechanics.

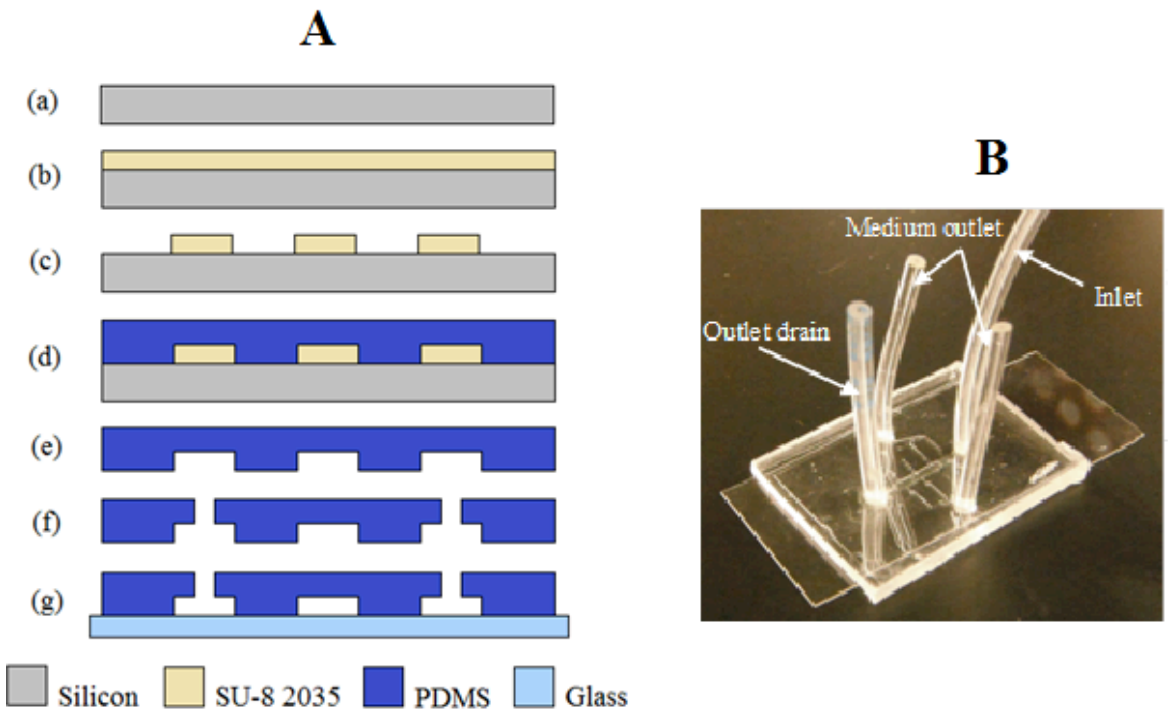

Figure 9. LOC fabrication. (A) (a) Schematic representation of a LOC: Silicon wafer standard clean, (b) SU-8 2035 Photoresist spin coating, (c) Lithographic patterning and photoresist development, (d) PDMS pouring and curing, (e) PDMS pouring and curing, (f) Fluidic access punching, (g) PDMS-glass bonding. (B) Fabricated LOC on a cover slip. Image is from Agudelo *et al*. (2014)

The fabrication of the LOC is explained in detail by Agudelo *et al*. (2014). Briefly, the LOC was designed using computer-aided design (CAD) and the design was transferred to a transparent film using digital printing or to glass using DWL lithography. To make a mold for the LOC, a silicon wafer was coated with the negative photoresist S8 to the desired thickness (usually 80 μM), covered with the film or glass pattern and exposed to UV light, and developed. A mixture of PDMS base and curing agent were poured on the resulting mold. After curing, the PDMS was removed from the mold and inlet and outlets were punched. A glass coverslip was then bonded to the device.

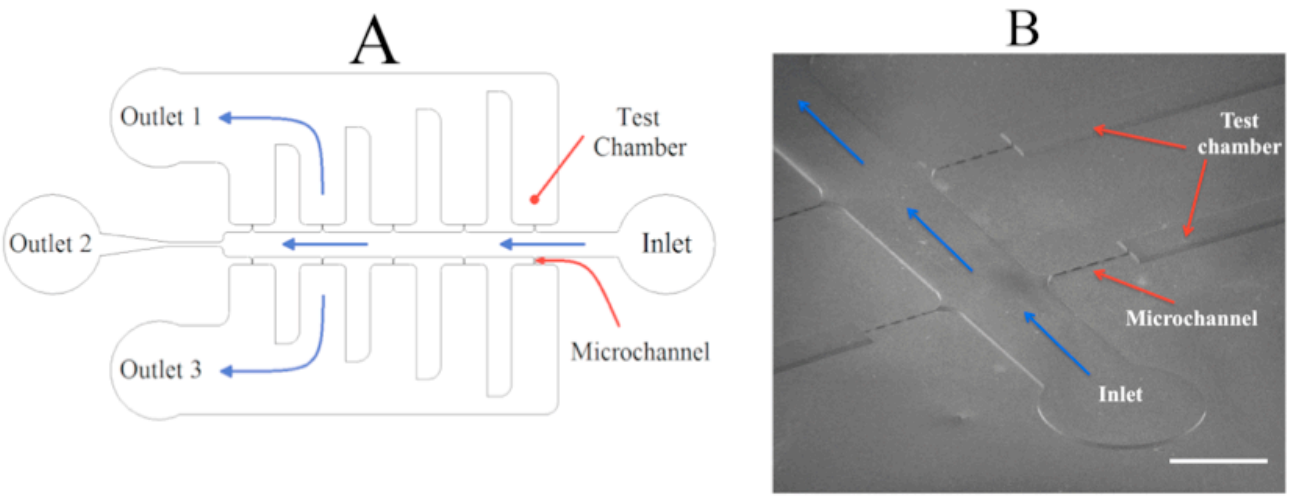

Figure 10. Presentation of LOC. (A) Schematic illustration of basic design for microchannels (LOC). (B) Scanning electron microscopy of LOC for narrow spaces. Pollen grains and medium are injected through the inlet tube. Untrapped pollen grains exit via outlet 2 and growth medium flowing through channels exits via outlets 1 and 3. Scale bar for (B) is 1mm.

The general design of the microfluidic network of the TipChip is explained in detail in Agudelo *et al* (2013, 2014) and Sanati Nezhad *et al* (2013a, b and d). The microfluidic network comprises a distribution chamber for injected pollen grains, and microchannels along which pollen tubes grow (Figure 8, provided by Agudelo *et al*, 2013). To ensure normal grain germination any mechanical obstacles are placed a minimum of 100 µm from the microchannel entrance.

Chapter 2: Invasive force

Amir Sanati Nezhad and I did the experimental work for this chapter and our data were published in PNAS (2013a), Royal Society of Chemistry (2013), and Biomedical Microdevices (2013). All the tests and experiments relating to the mechanical behaviour of pollen tubes during passage through narrow gaps were done in our laboratory at IRBV, The images were analyzed using ImageJ software in order to measure the changes in diameter of the pollen tube. Amir Sanati Nezhad did the chip design, most calculations and the modeling.

Summary

The growth of the pollen tubes inside the stylar transmitting tissue of the pistil has been studied from the point of view of the guidance signals emitted from the sporophytic pistillar tissues and female gametophyte (Yetisen *et al.,* 2011; Higashiyama and Hamamura, 2008). Since the pollen tube meets different types of cells, from dry stigma to the stylar transmitting tissue, it has to invade and penetrate inside the apoplast of all these cells to finally reach the surface of ovule (Lord and Russell, 2002; Cheung and Wu, 2001; Esau, 1977). The mechanical behaviour of pollen tubes during growth is not well understood. To determine the invasion force of the pollen tube, we used the novel technology of lab-on-chip (LOC) as *in vitro* condition to mimic the *in vivo* situation. In this study our model system is the pollen tube of *Camellia japonica*. Our results showed changes in growth velocity, when pollen tubes passed through narrow spaces during penetration. Also during invasion, the time necessary to pass the obstacle increased with decreasing the available space.

2.1. Introduction

Tip growing cells such as neurons, pollen tubes, root hairs and fungal hyphae have different responsibilities ranging from creating contacts between cells (neurons), transferring water and nutrients (root hairs and fungal hyphae) to delivering the male gametes to the recipient ovule (pollen tube). All of these tip-growing cells must overcome mechanical obstacles of neighbouring living tissues and penetrate and invade this extracellular substrate. This challenge is generally met either by producing digestive enzymes or other softening and dissolving agents against mechanical barriers, or by mechanical forces to push, penetrate or displace the obstacles. Animal and plant cells produce invasive forces in different ways, due to the fundamental differences in cellular architecture. In animal cells, the force required for cell invasion and migration can be produced either by cytoskeletal motor proteins (Ishijama, *et al*., 1991) or cytoskeletal filament polymerization (Theriot, 2000; Cojoc, *et al*., 2007). In contrast, plant and fungal cells use their internal turgor pressure to exert this invasive force.

The cellular envelope in plants and fungal hyphae is made of polysaccharide cell wall, whose mechanical deformation is required for morphogenesis to occur. The cytoskeleton controls the morphogenesis of the plant and fungal cells by regulating the deposition and assembly of cell wall components (Smith and Oppenheimer, 2005). Unlike in animal cells the cytoskeletal polymerization activities are not directly involved in generating growth and invasive forces (Money, 1997). Therefore, the only source of power for deformation of the cell wall is that of the turgor pressure (Schopfer, 2006). This power is exerted both on the cell's wall but also on the surrounding matrix. The range of turgor pressure in tip growing cells has been measured to be between 0.4 and 0.8 MPa in fungal hyphae (Lew, 2005; Howad and Valent, 1996) and 0.1 to 0.4 MPa for pollen tubes (Benkert *et al*., 1997).

In fungal hyphae, already hundred years ago researchers have investigated invasive force and the mechanism of growth. Miyoshi (1895) was able to quantify the fungal hyphae invasive force

exerted by creating a mechanical resistance using a gold membrane. After more than a century, Bechinger *et al* (1999) used an optical waveguide, Money (2001) used a strain gauge, and Wright *et al* (2005) used optical tweezers and beads that would be pushed by the growing force of hyphae to determine the invasive force in tip growing cells. Since the waveguide method requires the tight adherence of the cell body to the surface this technique cannot be used for the hyphae and most other tip-growing cells. Conversely, the ability of plant tip growing cells to invade has not been quantified. Pollen tubes have been studied by exposing them to stiffened agarose with different concentrations (our unpublished data), but for none of the plant tip-growing cells quantitative values for the invasive force have been determined. The disadvantage is the softness of agarose that allows the pollen tube to elongate inside agarose easily. In addition, the physical properties of agarose vary based on the percentage of the agarose, the brand and whether it dried out. Therefore it can affect the results, where the invasive force differs in repetitive experiments.

To address this lack of knowledge in the plant tip-growing cells, we used the pollen tube as a model system, since it has the fastest growth among plant cells, and its responsibility as central key for sexual reproduction is based on its invasive life style. In higher plants, the fertilization and seeds setting is a fundamental process in reproduction, in which the pollen tube plays an essential role by linking the two sexual partners through the stylar tissues of the female plant organs. The distance between the stigma and the ovule differs depending on the species and can be tens of centimeters. Therefore, the speed of pollen tube growth is an important selection factor for successful fertilization. As a result the pollen tube growth rate can be up to 1 cm/h (Taylor and Hepler, 1997; Williams, 2008). On its path toward the ovule, the pollen tube has to invade and find a way through the structure of the pistillar tissues. Once the pollen grain has attached to the stigma, it forms a tube, which elongates and starts to penetrate through the stylar tissue of either hollow or solid style, depending on the species. In the case of a solid style, a

cellular mass of transmitting tissue fills the stylar canal. This canal links the stigma to the ovary (Erbar, 2003; Palanivelu and Tsukamoto, 2011). When the tube reaches the ovary, it is attracted by the signals released by the female gametophyte, but it has to pass several barriers such as the internal surface of placenta, funiculus, and finally the micropylar opening to the ovule (Figure 4). To release the male gametes inside the female gametophyte for fertilization, the pollen tube crosses the tissue layer around the female gametophyte and reaches the synergids next to the egg cell (Berger *et al*., 2008). Transmitting electron microscopy has revealed that the space between the transmitting tissue cells is very narrow (Uwat *et al*., 1980; Lenon *et al*. 1998), and thus likely represents a mechanical obstacle. Pollen tube elongation can be facilitated by secretion of softening enzymes that digest the apoplast of the invaded tissue. Depending on the species, these enzymes are produced either by the pollen tube (Raghavan, 1997) or the pistillar cells (Gasser and Robinson, 1993) in the transmitting tissue (Wang *et al*., 1996). However, none of these procedures completely liquefies the pathway for the pollen tube and mechanical obstacles remain. Therefore, the pollen tube needs to apply an invasive force and we modified the earlier LOC, TipChip, to measure the ability of pollen tube invasion (Agudelo *et al*., 2012; Agudelo, *et al*., 2014).

In this particular TipChip developed for invasion studies, pollen tubes are directed to grow inside microchannels containing mechanical obstacles along the path. This current set-up is designed to measure the dilating force the tube exerts on the substrate by placing the obstacles in oblique manner. This is different from the strain gauge, which measures the force at the front of the cell (Money, 2007). In the *in vivo* situation, this corresponds to the apoplast of stylar tissue, which forms narrow gaps. To imitate this, the microchannels are equipped with the series of differently sized gaps through which the tubes have to squeeze to continue growing (Figure 12). The mechanical properties of the PDMS (polydimethylsiloxane) material allow us to calculate the dilating force exerted by the pollen tube when it deforms the microgap sidewall.

Moreover, we were able to classify different types of behaviour of the pollen tube during elongating through differently sized gaps (Sanati Nezhad *et al*., 2013a).

2.1.1. Device design

To quantitatively assess pollen tube invasion, we used a modified version of the TipChip (Agudelo *et al.,* 2012 and 2013). The TipChip was designed to contain narrow microchannels with regularly spaced, narrow gaps (Figure 12). Different sizes for the gap were used to be able to match pollen tube behaviour with the relative size of the tube to the respective gap.

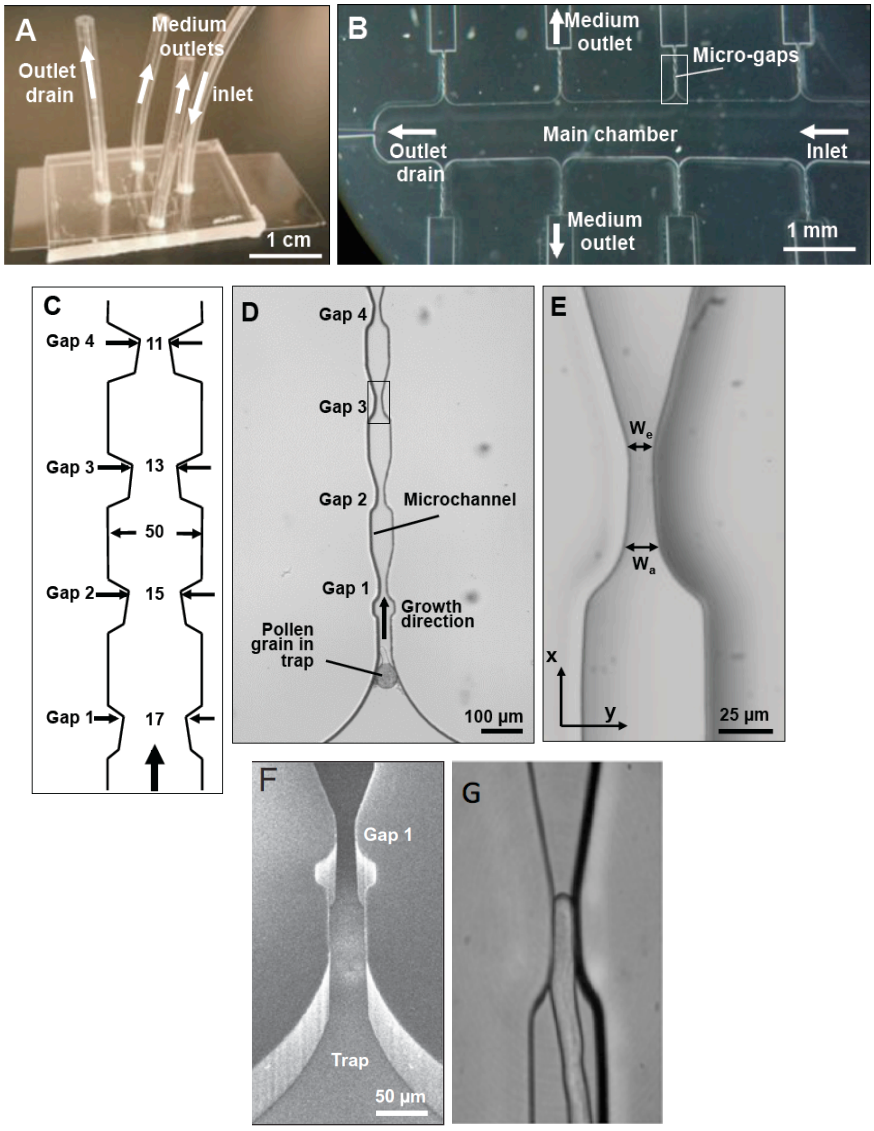

Figure 12. Fabrication of platform for measuring invasion by pollen tubes using microgaps. (**A**) General overview of principal TipChip illustrating arrangements of inlet and outlets. (**B**) Micrograph close-up of the microfluidic network geometry. (**C**) Schematic illustration of microchannel and serial microgaps. Numbers are in micrometers. The diagram is not to scale. (**D**) Bright field micrograph of the microchannel geometry demonstrating four gaps with a trapped pollen grain at the entrance. (**E**) Close-up micrograph of a microgap indicated in **D**, indicating openings of Wa and We. (**F**) Scanning electron micrograph of the microchannel entrance comprising the first microgap viewed from an oblique angle. (**G**) Micrograph of *Camellia* tube growing through a gap of 17 µm. The width of channel is 50 µm before and after the gap. This image is provided by Sanati Nezhad, *et al*. (2013a).

As shown in Figure 12 C and D, in this design the microchannels were setup to carry four consecutive narrow gaps where the normal width of the microchannel is reduced. The shape of these gaps are made of vertical clefts with the constant height of 80 μm and funnel shaped sidewalls, that become narrower along the distance of 40 μm, from the beginning width (W_a) to the narrowest part (W_e) (Figure 12 E). For the first gap, the size of 'W_e' was a little smaller than the average size of the diameter of a *Camellia* pollen tube (D1) and even smaller for the following gaps. Each gap was 2 μm narrower than the previous one. The two designs that we used here contained a gap of either 'We' = 17 μm or 16 μm, to the fourth gap with 'We' = 11 μm or 10 μm. In the y–z level, a microgap with 11 μm width has a rectangular shape of 11 μm x 80 μm (Figure 12 F).

When obstacles were perpendicular to the direction of growth, the pollen tube (Gossot and Geitmann, 2007) and fungal hyphae (Money, 2007) change their direction. Therefore, in our design we considered a funnel shape for the microgap to guarantee the pollen tube did not change its growth direction.

2.2. Material and methods

Pollen collection and germination

Pollen grains of *Camellia japonica* were collected from plants grown in the Montreal Botanical Garden and dehydrated in gelatin capsules on anhydrous silica gel overnight and stored at -20°C. Pollen grains were rehydrated in a humid atmosphere at room temperature for 30 min prior to *in vitro* culture. A very small amount (0.05 mg, average of 208 grains) of hydrated pollen grains was mixed with 1 ml of camellia growth medium. Camellia pollen growth medium contained 1.62 mM H_3BO_3 2.54 mM $Ca(NO_3)_2{\cdot}4H_2O$, 1 mM KNO_3, 0.81 mM $MgSO_4{\cdot}7H_2O$, and 8% sucrose (w/v). After allowing 1 hour for grains to start germination, the

pollen suspension was injected into the TipChip. To control fluid flow to the microfluidic network, growth medium was injected via a motor-controlled syringe (S200; KD Scientific, http://www.kdscientific.com/). The amount of liquid flow was 1 µl/min. The TipChip multichannel was placed on the microscope either after incubation time of one hour and a half, or right after injecting the pollen suspension. The samples were observed by microscope.

Fabrication of microfluidic device

As described in chapter 1, the TipChip is based on Lab-On-Chip (LOC) and MicroElectroMechanical Systems (MEMS) technology. The fabrication of microfluidic networks was made from polydimethylsiloxane (PDMS) using a silicon/SU-8 mold and was sealed with cover slip.

Microscopy

Samples were observed either with a Zeiss Imager-Z1 microscope equipped with a Zeiss AxioCam MRm Rev.2 camera and AxioVision Release 4.5 software or with a Nikon Eclipse TE2000-U inverted microscope equipped with a Roper fx cooled CCD (charged coupled device) camera and ImagePro (Media Cybernetics, Carlsbad, CA) software.

Bright-field imaging was performed on an Olympus BX60M bright-field microscope equipped with a Nikon Coolpix 4500 camera and a Nikon Eclipse 80i inverted microscope equipped with infinity 1 digital CCD camera and infinity analyzer software. Nomarski and fluorescence microscopy were performed on a Zeiss LSM 510 META confocal laser-scanning microscope using a Plan Apochromat 63x oil immersion objective with numerical aperture 1.40 and differential interference contrast.

Agudelo *et al*. (2013) performed scanning electron microscopy on gold/palladium-coated samples using an FEI Quanta 200 3D operated at 15 kV.

2.3. Results and Discussion

Fabrication of the microfluidic platform and invasion of narrow spaces

The success of pollen tube invasion depends both on the force it is able to exert and the flexibility it displays to enter narrow spaces. To assess this latter question, we devised a microchannel that exposes an elongated pollen tube repeatedly to stiff, narrow openings (Figures 10 A and B). In the present device (Figures 10 and 9), the gaps are elastic and relative short in length to allow for recovery. To pass the gaps, the pollen tube needs to change its diameter or deform the gap. The width of the channel changes between 50 μm in the wide portions to a series of gaps with decreasing diameter from 17 μm, 15 μm, 13 μm, to 11 μm. The gaps are 40μm in length and they are narrow only in horizontal direction, there is no limitation in vertical direction. We measure the growth rates before, during and after passage through a gap to determine how this parameter is affected by the geometrical constraint. In addition, this device permits us to establish the minimum size of the gap that pollen tube can pass through and whether the pollen tube returns to its original tube diameter after passing through the gaps.

The elongating pollen tube hit the sidewall of the microgap at the start point of S (Figure 13 A). To proceed through the microgap, the tubes could either perform a dilating force against the sidewalls and deform the microgap, or could change perpendicularly to the long axis of the tube in the y direction, to become a narrower tube or both. At the exit of the microgap (point E on Figure 13A) the microchannel widened to return to the standard width of 50 μm (Figure 14 C, D, and H). Depending on the relative sizes of pollen tubes and gap, different interactions were observed. When pollen tube passed through gaps, it caused the deformation of the PDMS sidewall at the narrowest part of the gap exit from its original width W_e' (minimum gap width before pollen tube enters the gap) to 'W_f' (minimum gap width in the presence of the pollen tube) (Figure 13B). When 'W_f' equals 'W_e', no deflection of the sidewall occurred and instead

the pollen tube decreased its diameter, to fit the gap size. In contrast, when 'W$_f$' equalled 'D$_1$' (D$_1$, width of pollen tube before entering the gap) there was full deflection of the sidewall and there is no change in pollen tube diameter.

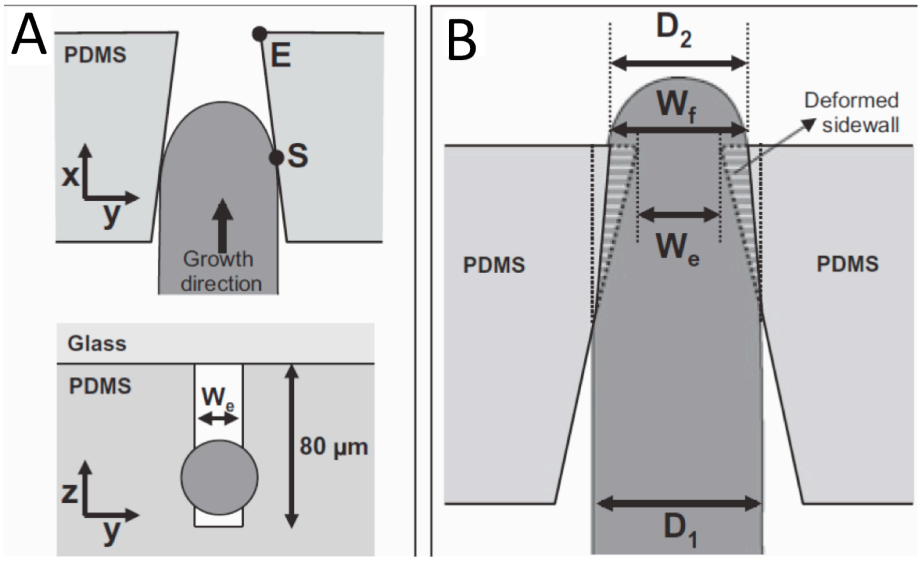

Figure 13. Schematic presentation of interaction between pollen tube and microgap. (**A**) Representation of interaction between an extending pollen tube (dark gray) and a microgap viewed from above. There is a first contact of the pollen tube with both funnel sidewalls forming the microgap at the point S. The lower schema represents the microgap in rectangular shape as an opening (white) in the PDMS material (light gray), viewed in the direction of pollen tube growth. (**B**) The passage of pollen tube through the microgap deforms the PDMS sidewalls of the gap at the narrowest part from W_e to W_f. During its passage through the gap, the pollen tube reduces its width from the original size of D1 to D2 temporarily, but after passing the gap it comes back to its typical width. Image taken from Sanati Nezhad *et al.* (2013a).

Pollen tube navigation via microgaps

We determined the average growth rate of *Camellia* pollen tubes to be between 4-11 µm/min (0.067-0.2 µm/sec) inside the microchannels. For the pollen tubes that were not subjected to mechanical forces by microgaps, the diameter varied between 13 to 21 µm. Thus, some pollen

tubes were not constrained by the first or second gaps. We observed that more than 90% of the pollen tubes were able to pass through the first two microgaps (17 μm and 15 μm) without interference with growth velocity. Four different types of pollen tube behaviours upon the meeting narrow gaps were detected: (i) Pollen tube diameter did not change visibly during passage through the gap, but PDMS sidewall was deformed (n = 20) (Figure 14C). (ii) The shape of pollen tube changed when it passed through the gap (n = 5) (Figure 14G). The observation of reduced width of pollen tube by microscopy could represent a true decrease in diameter or a local shape change from round to oval. Following this temporarily reduction in the width the cell typically returned to its original width, after entering into a wider section of microchannel (Figure 14 B). However, in numerous instances a significantly diameter wider than the original diameter was observed after gap passage (Figure 14 C). This widening was typically temporary and the tube diameter eventually returned to its original dimension. (iii) The pollen tubes burst after passing the gap and at the moment of entering the wider portion of microchannel (n = 8) (Figure 15 A). (iv) the pollen tubes stalled inside the gap (n = 10) (Figure 14 E).

The observation of different types of behaviours confirms that the elasticity of the PDMS is an appropriate material in our TipChip system, to measure the mechanical forces exerted by *Camellia* pollen tubes. If the PDMS were too soft to force shape changes or to stiff to be deformed by tube passage, the assessment of the dilating force would be impossible.

Since there is variety in the tube diameter, we plotted tube diameter against respective gap with and marked the type of behavior (Sanati Nezhad *et al*., 2013a). This revealed that a pollen tube diameter/gap size ratio of ≤1.20 was correlated with the gap passage without any effect on either the shape of the tube or growth rate. On the other hand, tube growth stopped when this ratio was >1.33. With the ratio between 1.20 and 1.33, the pollen tubes passed through the gap, but either burst after exiting the gap or displayed a temporary diameter change. Those tubes that

were able to pass the gap successfully, showed reduction of growth rate during contact with the narrow spaces (Figure 13B). Following emergence from the gap the pollen tube growth rate recovered (Figure 13) (Sanati Nezhad *et al*., 2013a).

We further analyzed the variation of pollen tube behaviour during gap passage. Some of the pollen tubes easily passed all the gaps even the fourth, most narrow one (n=11). Some of the pollen tubes passed the first and second gaps easily, but slowed down at the third and fourth gap (n=10). Some pollen tubes could not pass the fourth gap; they either burst (n=9) (Figure 15 A and C) or stalled while cytoplasmic streaming continued (n=8) (Figure 15 D). In some cases, after passing the second, third or fourth gap the pollen tube burst (n=12). In this situation, prior to bursting the growth rate of the pollen tube was significantly slowed down during passing the gap. However, in most of the time pollen tube was able to pass through gap either by decreasing its diameter in width (Figure 15 B) or by pushing the walls toward the both sides and opening the gap (Figure 15 E). We measured the growth rates before, during and after passage through a gap (Figure 14). Our data showed that the growth rate of pollen tube decreased from 0.18 μm/sec to 0.09 μm/sec and to 0.062 μm/sec inside the gaps, when the diameter of the gaps reduced from 15 μm (Figure 14E) to 13 μm (Figure 14G) and 11 μm, respectively (Figure 14J).

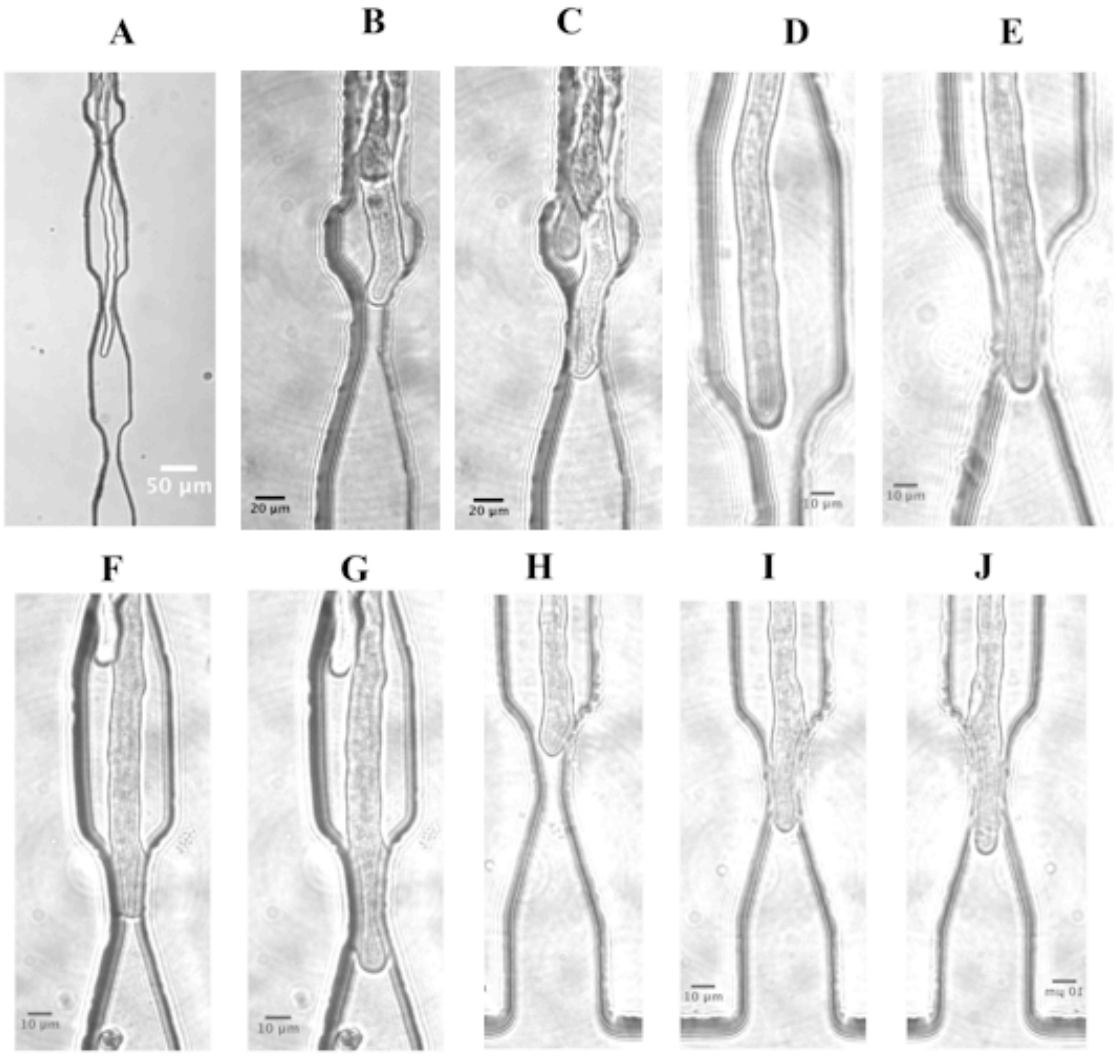

Figure 14. Growth of *Camellia* pollen tube through micro gaps. (A) Overview of microchannel with several gaps, (B) Pollen tube enters into the first gap (at 3420 sec; Reference time is 0), (C) Pollen tube passing through the first gap while pushing against the gap walls (3900 sec); a second tube is visible, (D) Pollen tube before entering the second gap (350 sec) (E) the same pollen tube passing through the second gap of the same microchannel (660 sec), (F) Different pollen tube in another channel passing at the third gap (3100 sec), (G) The diameter of pollen tube changed when it was passing through narrower gap, compare to second gap 'E' (3370 sec), (H) A pollen tube at the entrance of the fourth gap (2310 sec), (I) when passing through fourth gap (2770 sec), (J) and when exiting the gap (2940 sec). Scale bars: (A)= 50 µm; (B-J)= 10 µm.

In one instance, the pollen tube stopped for 29 minutes in the gap with neither bursting, nor swelling (Figure 15 D). However, we were able to observe the cytoplasmic streaming inside the pollen tube as well as the male germ unit consisting of the two sperm cells and the vegetative

nucleus. The male germ unit kept its distance from the tip of pollen tube constant at 93 μm for the entire 29 minutes. The ability to observe intracellular organelles with the 20X objective lenses was one of the great advantages of current design of the LOC device.

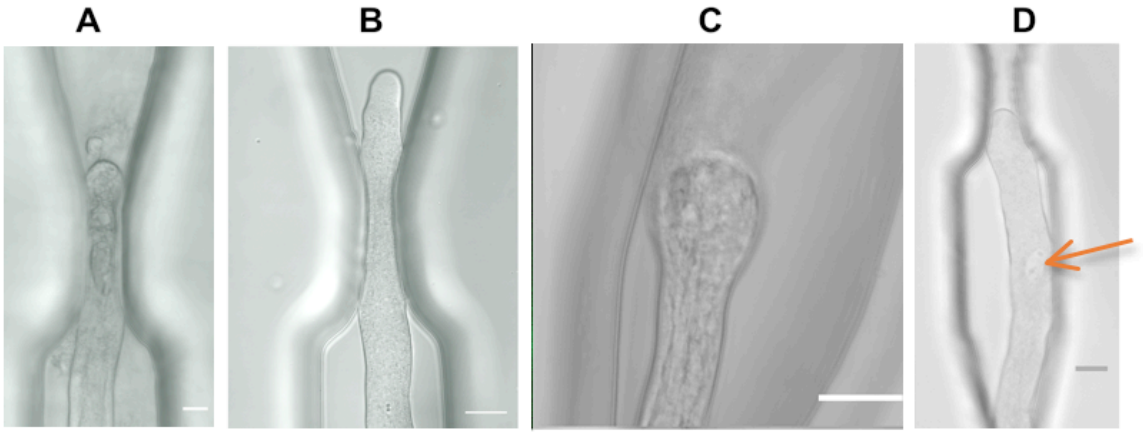

Figure 15. Different behavior of *Camellia* pollen tube during passage through micro-gaps. (A) The pollen tube is stuck at third third gap and burst after 1 minute, (B) Reduction of the pollen tube width at the gap number 4 and continued growth after passage. (C) A pollen tube that burst after passing the second gap. (D) A pollen tube stalled in the second gap for 29 minutes. Orange arrow indicates the vegetative nucleus inside the pollen tube. Bars = (A) 5 μm, (B) and (C) and (D) 20 μm.

Effect of mechanical constraint on growth rate

The data had shown that upon decreasing of gap size, the time required for a pollen tube to pass the obstacle was prolonged. The growth rate decreased most dramatically at the third and fourth gaps (Figure 16).

The growth velocity decreased from the first to fourth gap, in which the length of pollen tube increased in longer time (Figure 16).

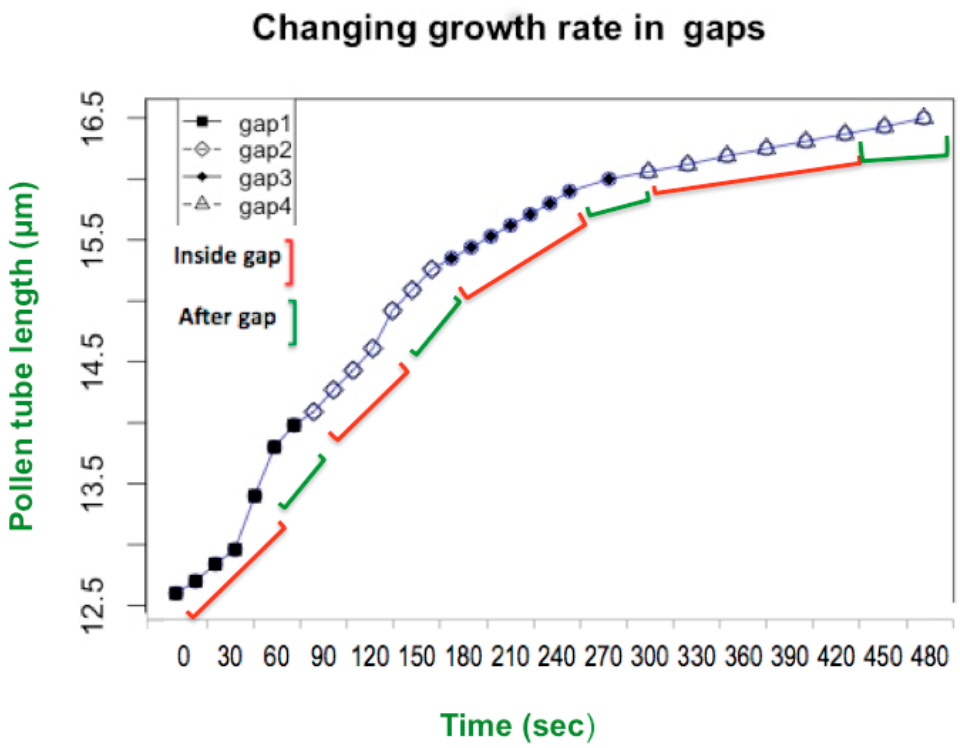

Figure 16. Changing the growth velocity of *Camellia* pollen tube in the micro gaps. The growth rate during gap passage is lower than between gaps and decreases with decreasing gap width. The gaps are indicated as: gap#1 (filled square), gap#2 (empty square), gap#3 (filled circle) and gap#4 (empty triangles). The growth rate of pollen tubes, when the tube is inside the gap (red closed parentheses), and recovered after the gap (green closed parentheses).

2.4. Male Germ Unit

The pollen tube male germ consists of a vegetative nucleus and two sperm cells, which are surrounded by a double membrane (Figure 18). The components of this unit are in physical connection and move forward along the growth direction of pollen tube microtubule cytoskeleton of the vegetative cell (Åström *et al.,* 1995). From our study we determined that the vegetative nucleus of *Camellia* pollen tube always stayed close to the tip at the distance of ~60–80 µm from the apex, and the sperm cells kept following the vegetative nucleus with a distance of between 120 µm and 155 µm from the tip. During unchallenged growth, they stayed

at these distances but when growing through a narrow gap the vegetative nucleus had difficulty to follow the tip of pollen tube (Figure 17). In this situation, the nucleus had to rotate or turn to pass, which likely takes more time and its distance to the apex of pollen tube increased. After passing the gap it speed up to reach the original distance to the tip. In the case of bursting tube following gap passage, the male germ could be trapped before the gap and as a result was not ejected (Figure 17).

Using our advanced system of LOC, we were able to show that narrow spaces affected the behaviour, velocity and passing time of pollen tube. Although the morphogenesis and growth rate regulating of pollen tube both depends on the mechanics of the cell wall, the driving force for cellular expansion and pistillar invasion is the turgor pressure (Winship *et al*., 2010 and 2011). In addition, changes in the osmotic pressure of the surrounding medium can modulate the growth behaviour of pollen tubes (Zerzour *et al*., 2009; Chebli and Geitmann, 2007). In future studies we therefore are very interested in investigating how a modulation in the turgor pressure affects the pollen tube's invasive force and its capacity to pass the narrowing gaps.

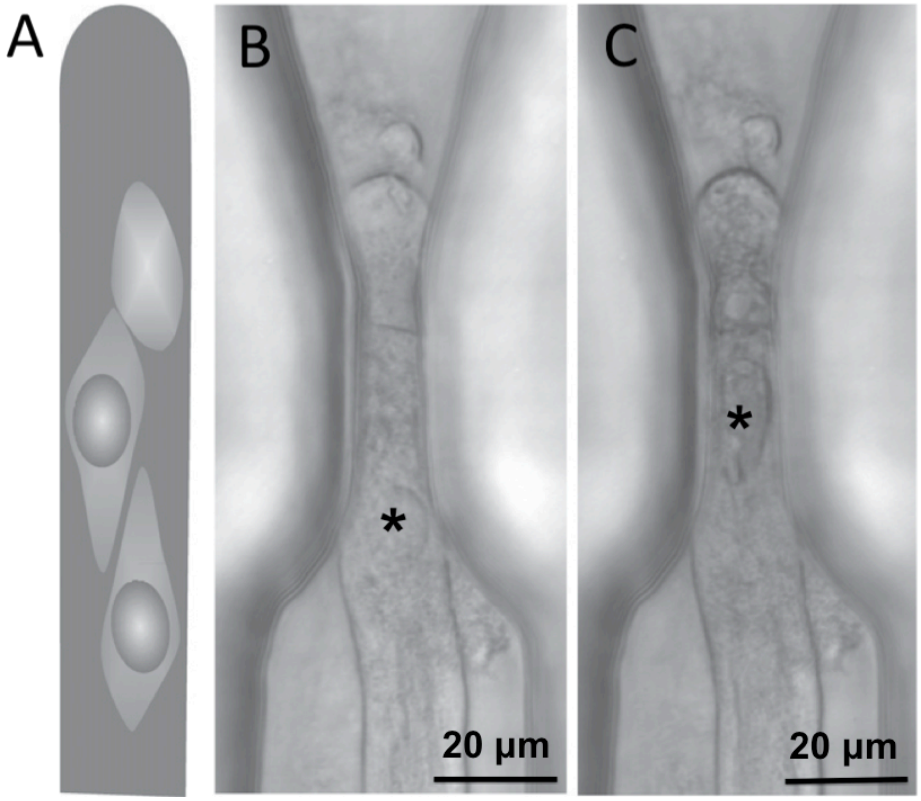

Figure 17. Passage of the male germ unit through a microgap. (A) Graphic presentation of the male germ unit consisting of the vegetative nucleus and sperm cells, with their normal distances to the tip in case of the *Camellia* pollen tube. Note that objects are not to scale. (B and C) Showing the bright field micrographs of a burst pollen tube during gap passage. Because of the pressure release during bursting, the male germ unit is pushed through the gap and the vegetative nucleus (*) becomes slimmer but stalls inside the gap without discharging. Image from Sanati Nezhad *et al*. (2013a).

2.5. Calculation of the dilating force of the pollen tube

Finite Element Simulation

Pollen tubes with a diameter ≥1.2 times larger than the gap managed their passage by altering their shape, and those with a diameter between 1.0 and 1.2 pushed the sidewall of PDMS for penetrating the gap without changing their shape (Figure 18A). This explains the ability of pollen tube in application of dilating forces in radial direction to maintain its cellular shape against the mechanical resistance from the pistillar tissues. To quantify this force, finite element analysis was used, as described in detail in Sanati Nezhad *et al*. (2013a). The force the tube would need to deform the PDMS side walls and the modeling was based on tubes that did not change diameter during gap passage. The simulations showed that a contact pressure of 0.15 MPa was able to deflect the microgap 1.5 μm at the narrowest point of the gap. Using the magnitude of the contact surface btween tube and wall of 98 μm^2, this enabled calculating the force exerted on the side wall to be 14.7 μN.

2.6. Discussion

The mission to invade a surrounding substrate or tissue is a crucial ability of tip-growing cells such as neurons, fungal hyphae, root hairs and pollen tubes, regardless of the purposes of this activity. The pollen tube uses the invasive behaviour for transporting the male gametes to the ovary. Besides the application of invasive force, the pollen tube has to protect the male germ unit during transportation. The tubular shape of the tube also is essential, since bending or folding of the tube could potentially prevent the transit of the sperm cells. Therefore, pressure from inside is required to prevent the tube collapsing under the pressure of the external environment. Since the pollen tube is not a solid material (like a needle), it could be compared to a balloon catheter (used in angioplasty for opening blocked arteries). Thus, the investigation of pollen tube behaviour when facing an obstacle persuaded us to investigate the interaction of elongating tubes with structural materials *in vivo* such as those inside the apoplast of the pistillar tissues. Our observation confirmed that the pollen tube penetrated the obstacles when possible, rather than avoiding them by changing growth direction. Our results suggest that a pore with reasonable size and elasticity will be displaced during pollen tube passage without affecting pollen tube diameter. In contrast, narrower openings might oblige the pollen tube to reduce its width. Moreover, very narrow openings are likely to prevent the passage of the male germ unit even if the growing apex passes.

The diameter of the pollen tube varies significantly between species. For example, the pollen tube diameter in *Arabdopsis* is 5 μm, and in *Camellia* is 17 μm. However, within a particular species, the variation in diameter is small. After gap passage *Camellia* pollen tubes rapidly returned to their typical diameter suggesting the existence of internal control of shape. This makes sense as this ensures efficient transportation of the male germ unit without getting trapped. While cell shape formation in the pollen tube has been modeled (Fayant, *et al*., 2010; Kroeger and Geitmann, 2012) an explanation for the size differences between species is still

elusive.

The occasional bursting of pollen tubes after gap passage was reminiscent of the release of the sperm cells *in vivo*. Once the pollen tube enters the female gametophyte, the two sperm cells get liberated via pollen tube bursting. Hence, bursting is a critical, it is the last event in the pollen tube's life and it ensures successful fertilization. Amien *et al*. (2010) and Berger *et al*. (2008) report various intergametophyte agents responsible for signalling and guiding the pollen tube toward the ovule, but the physiological mechanism involving pollen tube bursting and sperm cell release is poorly understood. Our study suggests that possibly the discharge trigger has a mechanical component. The trigger could be represented in form of the micropyle, the opening in the teguments covering the ovule, the nucellus, the layer surrounding the female gametophyte, or the filiform apparatus of the synergids (Figure 5). However, some aspects of our study speak against this hypothesis. In our *in vitro* setup bursting happened within a size ratio range of 1.20 and 1.33. Tubes smaller than 1.2 times the gap can pass through easily without bursting and when they are wider more than 1.33x they stall. This leaves a very narrow size range that would be triggered to burst by a particular micropyle. Whether this is therefore biologically relevant remains to be proven and the investigation of potential proteic or chemical triggers remains important (Berger *et al*., 2008; Amien *et al*., 2010). Whether or not the mechanical trigger is biologically relevant for sperm cell release *in vivo*, our findings confirm that plant cells respond to mechanical triggers.

The microgaps of the TipChip are made with a specific geometry and the mechanical properties of the gaps are known. This permitted us to use finite element methods to calculate the effective pressure applied by the pollen tubes onto the gap walls. To deform the PDMS at the narrowest point of the gap, the pollen tube applied a maximum pressure of 0.15 MPa on the sidewall of the gap. Regardless of the direction of force applied by the pollen tube, whether horizontally to the gap or in the direction of growth, the turgor pressure produces this force.

While the average turgor pressure in lily pollen tube is reported to be 0.2 MPa (Benkert *et al*., 1997), no values are available for *Camellia*. However, the dilating pressure we calculated is close to the value of the lily turgor albeit a bit lower. This is consistent with the fact that the cell wall absorbs some of the pressure. In fungal hyphae only 10% of the total turgor pressure seems to be available for invasion (Money, 2004 and 2007), but our data suggest that in pollen tube this percentage is higher. The magnitude of the force exerted by the pollen tube confirms that invasion in this cell is driven by the turgor rather than by cytoskeleton mediated forces which would be much smaller.

The softer cell wall at the very tip of the tube (Fayant *et al*., 2010) ensures the formation of a cylindrical structure but also causes that higher forces are applied onto the growth substrate in the direction of growth than in lateral direction. However, additional investigation and a variety of mechanical methods are required to confirm this (Geitmann, 2006).

Interestingly, we observed that during gap passage the pollen tube is able to modulate the invasive force it exerts, since despite increasing impedance the growth rate remained stable. In the time sequence plots for the growth rate (Sanati Nezhad *et al.,* 2013a), the rate was reduced upon first contact of the pollen tube with the gap sidewalls, but subsequently did not drop further. The modulation in growth force could be achieved either by modulating turgor pressure or by modulating the stiffness of the cell wall. The bursting of the pollen tube after gap passage could potentially be caused by either mechanism. However, our previous finite element model (Fayant *et al*., 2010) indicates that turgor increase would not cause an alteration in tube diameter whereas a change in cell wall stiffness would. As shown in Figure 15B, the tube widens after passing the gap thus confirming that the cell wall stiffness is the parameter that is modulated to adapt the invasive force to the increasing impedance. Future studies will focus on the role of the osmotic value of the medium and the turgor pressure of the cell in invasion and

penetration, in addition to studying the role of the actin cytoskeleton and vesicle trafficking on directional growth behaviour.

Chapter 3: Compatibility of LOC devices for high-resolution microscopy

Summary

Tip growth is sustained by extremely rapid and efficient intracellular transport of cell wall material to the growing tip. Therefore, analyzing the dynamics of intracellular transport in these cells can reveal important details about the growth and steering mechanism. In particular, it would be interesting to document changes to the intracellular transport when cells are either passing through narrow spaces or changing the orientation of their directional growth. In the *in vivo* situation, a change in growth direction may be the result of different reasons - either because the cell faces an obstacle or because it actively follows guidance signals. The simultaneous monitoring of the growth behaviour and the intracellular processes is an excellent application for the TipChip as it requires high-resolution microscopy in combination with a mechanical and geometrical test setup. Here we tested the compatibility of our advanced microfluidic device with high-resolution optical microscopy by observing elongating pollen tube within the LOC using confocal laser scanning microscopy and Nomarski (differential interference [DIC] contrast) optics. DIC optics is not compatible with plastic material such as petri dishes, because of their birefringence, but the materials used for the TipChip system do not pose optical problems. To test fluorescence imaging we labeled the endomembrane system of the pollen tube using the styryl dye FM1-43. We noticed that this dye adheres to the sidewalls of the PDMS microfluidic network. This property of the dye might be useful for imaging the network geometry with necessitating bright-field optics.

3.1. Introduction

Observation of cellular growth and interaction with the microenvironment is one of the applications of the TipChip that we envisage. The tip-growing cells elongate to reach either their purpose or destination. On their path they have to invade and penetrate surrounding area containing different types of either biotic or abiotic materials and obstacles. The tip-growing cells of eukaryotes are root hairs, fungal hyphae, pollen tubes, and neurons. Fungal hyphae grow to reach for nutrients and water inside the soil or host plants or animals (Harris, 2008). Root hairs penetrate the soil to take up water and minerals and transfer them to the vascular network of the root to nourish the plant (Haling *et al*., 2013; Takemot *et al*., 2006). Cancer cells penetrate and pass through the surrounding tissue to enter and exit blood or lymph vessels. This way they distribute to remote locations and propagate inside another organ to develop metastases (Yamaguchi *et al*., 2005; Kumar and Weaver, 2009). The extension of neuron in form of axons, serves to generate synapses to make connections with either another neuron or a target cell. An axon elongates via the extension of its grown cone composing filopodia (finger-like shape) and lamellipodia (extensional structure) (Haydon, 1988; Dickson, (2002); Dent and Gertler, 2003; Loudon *et al*., 2006). Pollen tubes grow toward the micropyle of the ovule inside the female stylar structure and it has to invade and penetrate and turn around obstacles on its way to finally reach its target (Taylor and Hepler, 1997; Lord and Russell, 2002; Geitmann and Palanivelu, 2007; Higashiyama and Hamamura, 2008; Yetisen *et al.,* 2011).

To understand how tip growing cells reorient their growth, various techniques have been used. In earlier studies in our lab, turning of the pollen tube was achieved by application of a global electrical field within a Petri dish (Bou Daher and Geitmann, 2011). However, this setup relies on immobilizing pollen in agarose, the control of fluid circulation was thus impossible. In the TipChip system, the pollen grains are immobilized at the entrances of microchannel, and liquid medium can be used while no agarose limits high-resolution imaging. High-resolution

imaging is necessary for example to study the intracellular transport processes in cells changing direction or being challenged by mechanical obstacles. During fertilization, the pollen tube follows the chemical signals emitted by the sporophyte and the female gametophyte and changes its growth direction multiple times (Higashiyama and Hamamura, 2008). Our TipChip device (Agudelo *et al.,* 2013; Sanati Nezhad *et al*., 2013a) is able to imitate certain aspects of the *in vivo* condition of the stylar tissue. It was suggested that a change of growth direction in the pollen tube requires a modulation in the delivery pattern of the secretory vesicles at the growing apex (Geitmann and Steer, 2006; Bou Daher and Geitmann, 2011). The transportation of vesicles is mediated by the actin cytoskeleton (Shimmen and Yokota, 2004), an important element that mediates the cellular response to an external signal. The actin cytoskeleton in the rapidly growing pollen tube cell is very dynamic and involved in the morphogenetic process. Earlier studies in the lab have shown the polymerization of actin cytoskeleton in the different cellular regions occurs at different rates in turning pollen tubes (Bou Daher and Geitmann 2011). Because of the involvement of intracellular transport processes in cellular morphogenesis, monitoring these processes (vesicle trafficking, actin dynamics) is vital for our understanding of the tip growth mechanism. Therefore, the visualization of labelled vesicles during reorientation using the LOC microdevices is one of the assays we would like to be able to perform. We therefore tested whether fluorescence imaging at high resolution is feasible using the TipChip. As a test object we observed elongating pollen tubes inside the different fabricated devices after labeling with styryl FM1-43 dye for for the visualization of endomembrane structures. We used confocal laser scanning microscopy and Normarski optics (differential interference contrast). Unlike birefringent materials such as plastic Petri dishes that prohibit the observation via Nomarski optics (Inoué and Sato, 1976; Friese *et al*., 1998), the TipChip performed fine for all imaging needs (Figure 19 A-C).

3.2. Material and methods

Microfluidic network design

CAD software was used to design the LOC. It was replicated using either digital printing onto a transparent film, or direct-write lithography (DWL) onto a glass mask (DWL 66FS; Heidelberg Instruments, http://www.himt.de/en/home/) (Agudelo *et al.,* 2012 and 2013). A negative photoresist, SU-8 (Micro-Chem Corp., http://microchem.com/) was used to fabricate the mold operating a photolithographic technique. Then the SU-8 was spin-coated on a 10 cm silicon wafers (WRS Materials, http://www.silicon-wafers.com/) to finalize the thickness of 80 µm. Two soft-baking phases of 5 min (at 65°C) and 10 min (at 95°C) on a hotplate prepared the SU-8 to be subjected to UV light by a photo mask. Then the SU-8 layer was post-baked with two steps for 5 min at 65°C and for 10 min at 95°C in a hotplate, and finally the SU-8 mold was developed. PDMS was mixed at a weight ration of 10:1 and poured onto the SU-8 mold. After peeling off the PDMS replica from the mold and punching the inlet and outlets, oxygen plasma bonding was used to attach this layer to a glass cover slip (Harrick Plasma PDC-001, http://www.harrickplasma.com/) for sealing (Bubendorfer et al., 2007). To visualize FM1-43 fluorescence, both 60X or 100X objectives of Zeiss LSM-510 META confocal laser scanning microscope along the excitation light at 488 and a 566 nm band-pass emission filter were used.

Pollen culture and germination

Pollen grains of *Camellia japonica* collected from a plant in the Montreal Botanical Garden, were dehydrated and stored on silica in gel tubes at –20°C until use. Before the experiment, few milligrams of the pollen were thawed and rehydrated in a humid chamber for 45 minutes. Then an average of 208 grains (0.05 mg of pollen grains) were suspended in 1 ml of liquid camellia growth medium (Bou Daher and Geitmann, 2011). *Camellia* pollen growth medium contained 1.62 mM H_3BO_3 2.54 mM $Ca(NO_3)_2 \cdot 4H_2O$, 1 mM KNO_3, 0.81 mM $MgSO_4 \cdot 7H_2O$, and 8%

sucrose (w/v). The pollen suspension was incubated in a humid chamber for an hour to germinate, and then was injected using a syringe into the TipChip. To control fluid flow through the microfluidic network, growth medium was injected via a motor-controlled syringe (S200; KD Scientific, http://www.kdscientific.com/). The amount of liquid flow was 1-2 µl/min. The LOC (TipChip multichannel) was placed on the microscope either after incubation time of one hour and half, or right after injecting the pollen suspension. The samples were observed by microscope.

Imaging

Bright-field imaging was done with an Olympus BX60M bright-field microscope (http://www.olympus-global.com/en/) equipped with a Nikon Coolpix 4500 camera (http://www.nikon.com/) and a Nikon Eclipse 80i digital imaging microscope system. Nomarski and fluorescence microscopy were performed on a Zeiss LSM 510 META confocal laser scanning microscope (http://corporate.zeiss.com/gateway/en_de/home.html) using a Plan Apochromat 63x oil immersion objective with numerical aperture 1.40 and differential interference contrast. For visualization of FM1-43 fluorescence, we used excitation light at 488 and a 566 nm band-pass emission filter. Scanning electron microscopy was accomplished on gold/palladium-coated samples using an FEI Quanta 200 3D (http://www.fei.com/) operated at 15 kV.

Vesicle labeling

The vesicles were labelled with the lipophilic styryl dye FM1-43 (Molecular Probes, Invitrogen). The pollen grains inside the device were allowed to germinate and grow for 40 minutes and then the FM1-43 dye was added to the growth medium at 160 nM for 30 minutes. Finally medium with no dye was allowed to flow through the device to remove excess dye. The dynamics of vesicles were monitored by time-lapse imaging using the Zeiss LSM 510 META Live Duo confocal microscope equipped with a LSM 5 LIVE, with the excitation light at 488

and a 566 nm band-pass emission filter.

3.3. Results

TipChip and high-resolution imaging with Nomarski and fluorescence microscopy

The vesicle cone is located at the very tip (apex) of the pollen tube, where the vesicles bring the required cell wall materials and vesicles that fail to exocytose return backward toward the centre through the tail of the vesicle cone (Figure 1). The location of the apical vesicle pool (Figure 19B, arrow) corresponds to the proximal end of actin fringe (Bove *et al.,* 2008) which is responsible for the delivery and targeting of vesicles carrying cell wall material (Taylor and Hepler, 1997; Geitmann et al., 2000; Kovar et al., 2000; Vidali et al., 2001). We tested the compatibility of our TipChip for high-resolution imaging by monitoring the vesicle cone in pollen tubes interacting with mechanical obstacles. For this experiment, a TipChip device with fourteen microchannels around a circular chamber was used (Figure 21A). This device contained four different types of microchannels: straight, spindle shaped, zigzag and a 90° turn. Preliminary observations showed the zigzag and 90° angled microchannels guided the pollen tubes to change their growth directions (Figure 21 A and B). The apical vesicle pool (vesicle cone) is clearly monitored with the high-resolution of confocal laser scanning microscopy (Figure 19B).

The use of FM1-43 dye allowed us to track and observe the vesicle cone at the very tip of pollen tube before and at the moment of turning. However, the dye also bound the PDMS of the channel walls (Figure 19C and 22D). We were able to observe the vesicle cone at the apex of the pollen tube in 2 out of 10 tubes, because of the high background fluorescence interfered with many of our observations. Higher amounts of FM1-43 did not improve the situation, since

the fluorescence intensity on the sidewalls of PDMS microchannels increased as well (Figure 19C and 22D).

In attempt to solve this problem I changed the procedure to adding the dye inside the TipChip 15 minutes prior the injection of the pollen grains. The dye continued to be added inside the device by flow-through for 15 minutes after the injection of pollen grains. Then I changed it for flowing the liquid growth medium without the dye, for the rest of the experiment. However, this situation did not solve the problem, even for an average time of 2 hours the detection and observation of the vesicles was impossible because the dye remained on the sidewalls of TipChip and made a high fluorescent intensity background. This fluorescence intensity interfered with the visualization of the fluorescent intensity of vesicle streaming and vesicle cone inside the tube. In addition, the adherence of dye to the sidewalls of TipChip may have reduced the amount of dye available for uptake by the pollen tube.

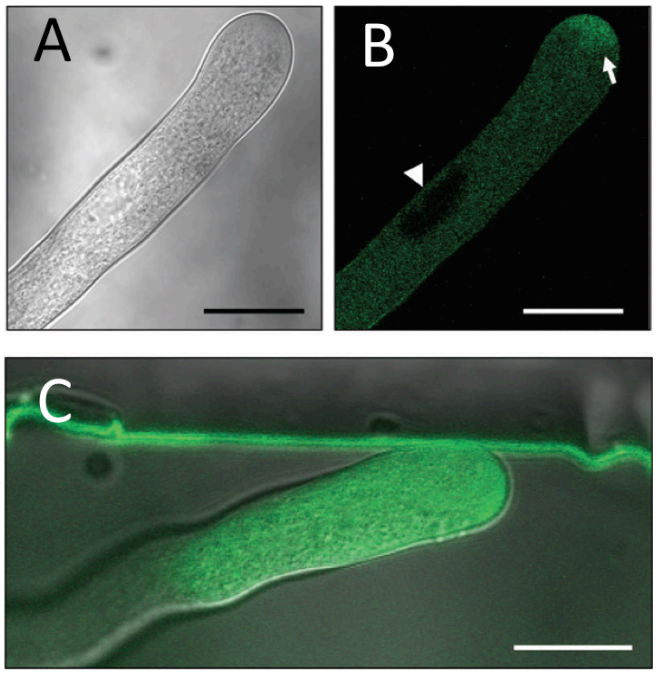

Figure 18. Testing of the TipChip with Nomarski optics and fluorescence. (A-C) The TipChip allows high-resolution imaging using Nomarski optics (A) as well as confocal laser scanning microscopy (B, C). The dye tested here is the styryl dye FM1-43, which is taken up by the pollen tube and labels endomembranes, particularly the apical vesicle cone (arrow), but not the generative nucleus (arrowhead). The overlay (Nomarski and FM1-43) (C) shows a different pollen tube in another microchannel, where the dye adheres to the PDMS sidewalls of the microfluidic device, a feature that may be useful for outlining the walls when bright-field optics are not available or desired. Scale bars = 20 μm.

3.4. Discussion

To move toward a better understanding of polar growth in tip growing cells, the development of a technique for measuring quantitative data is essential. Therefore, a standardized experimental setup could permit biologists to obtain data and results that can be compared quantitatively. Bio-micromechanical studies can help develop a new era of cell analysis and improve our knowledge of fundamental biological approaches that control tip growing cells at the apex, such as turgor pressure and cell wall mechanics.

Our advanced microfluidic-based platform developed for tip-growing cells represents a unique and powerful device, which can be used for pollen tube research, as well as fungal hyphae and other tip-growing cells. The biggest advantage of this device is its flexible design, which permits combining a variety of different structures. Therefore, the capability of monitoring the cell behaviour during growth and particularly the intracellular interactions are fundamental aspects for most of the applications. Monitoring cell behaviour during elongation and the effects of chemical agents as well as mechanical triggers of the TipChip device is in high demanded. Therefore, using high-resolution microscopicy to investigate pollen tubes during growth and elongation, and to assess its interaction with mechanical obstacles within the microfluidic device. To examine the compatibility of our device with high-resolution fluorescence microscopy, we designed a test based on the reorientation of the pollen tube tip. It is believed that actin-binding proteins, located at the subapical actin fringe of pollen tubes,(Vidali *et al*., 2001; Vidali and Hepler, 1997) regulate actin dynamics and in previous studies we have investigated actin depolymerizing factors ADF7 and ADF10 (Bou Daher and Geitmann, 2011). The location of the apical vesicle pool (Figure 19B, arrow) corresponds to the proximal end of actin fringe (Bove *et al.,* 2008), responsible for the delivery and targeting of vesicles carrying cell wall material (Taylor and Hepler, 1997; Geitmann *et al*., 2000; Kovar et al., 2000; Vidali et al., 2001).

The use of the styryl dye FM1-43 for labelling the vesicle membranes in the pollen tube revealed that the dye adheres to the PDMS sidewalls of the microfluidic network (Figure 19C and 22D). While the dye also labelled the vesicles at the pollen tube apex as intended, the high fluorescence intensity of the dye adhered to the sidewalls impaired the observation of the vesicle cone in the cell. For this experiment, after the injection of pollen grains inside the distribution chamber of device, 0.1 µl/ml FM dye suspended in growth liquid medium was used to stain the vesicles in the pollen tube. Because of the high amount of dye adhering to the microchannel walls in the previous test, the pollen grains were incubated with dye for 15 minutes after the injection and then the fluid was exchanged to liquid growth medium without dye. However, even prolonged rinsing was not able to remove the dye from the PDMS sidewall consistent with reports of PDMS that has been used in the studies for adhesion of the elements, platelets (Park *et al*., 1999) and cells (Kidambi *et al*., 2007; Fuard *et al*., 2008). PDMS, commonly used in biomedical applications, membrane technology, and microlithography, is an appropriate artificial substrate to culture and control the adhesion of variety of mamalian cells (Kidambi *et al*., 2007; Fuard *et al*., 2008). Park *et al.* (1999) used the advantage of PDMS devices for blood-contact in biomedical applications, where PDMS was coated with polyurethane (PU) and grafted monomethoxy poly(ethylene glycol) (MPEG). PDMS alone caused the high adhesion of platelets to the device. Kidambi *et al*. (2007) increased the adhesion of PDMS by building polyelectrolyte multilayers (PEMs) on PDMS surfaces. Faurd *et al,* (2008) linked the research area of sciences and microelectronics to study the effects of physical aspects of PDMS on cross-linker concentration, baking time on PDMS rigidity, hydrophobicity, relationship of hydrophobicity with cell surface and adhesion. They found that sufficient changing of physical chemistry of PDMS surface managed the fibroblast adhesion and the morphology (surface, polarisation and bulges) (Faurd *et al*., 2008). While inconvenient for the imaging of weakly fluorescent cells, this property of the dye may be extremely useful in order

to image the geometry of the microfluidic network when bright-field optics are either not available or not desired, or when the precise surface structure of the channels in 3D must be assessed.

6. Future work

We made a number of observations during our studies that open avenues for further investigations. We observed that *Camellia* pollen tubes are capable of growing in microchannels in the presence of aluminum and gold, but not with metallic copper (Agudelo *et al*., 2013). A fluid velocity of more than 30 $mm.sec^{-1}$ is inhibitory for the growth of pollen tube. We also found that pollen tubes, unlike other tip-growing cells, have no directional memory. However, in the contact with different concentrations of an attractant or repulsive agent, they can change their direction of growth. Unexpectedly, the pollen tube showed the ability to grow in air, when it was not surrounded by growth medium. For the biology of pollen, these recent discoveries are important for further investigations of tip-growing cells based on the microfluidic devices and MEMS techniques. Some of these largely preliminary observations are summarized briefly below.

6.1. The ability of pollen tubes to pass through the air–liquid interface and elongate in air

On the stigma surface, germination of pollen tubes starts in air. During the growth inside the long hollow style, as well as within the ovarian cavities, the pollen tube elongates through spaces that are at least partly filled with air, although fluid is likely to line the tissue surfaces (Felle *et al*., 2005; Hedrich *et al.,* 2001). Inside the TipChip the pollen tube normally grows

through completely liquid filled spaces. However, during our experiments occasionally air bubbles got trapped inside the microfluidic network. Generally, the tubes did not enter the air bubble and instead bypassed it (Figure 20A). However, occasionally, they were observed entering the bubbles. Although the pollen grain can germinate in the absence of liquid water, water vapour must be present to trigger germination (Ferrari *et al*., 1981). Pollen tube elongation is thought to require liquid water and ions, which enter the cell at the tube apex (Hepler *et al*., 2006; Zonia *et al*., 2006). To assess the pollen tube's capacity to grow in the absence of liquid water, we needed a specifically designed set-up. In the device designed for this purpose we allowed pollen tubes to germinate surrounded by liquid medium, but subsequently the pollen tube was guided to grow inside an air chamber (Figure 20 B and C). The entrance of air chamber was designed to be very narrow consisting of two parallel PDMS walls. This ensured that only the pollen tube entered the chamber but not the liquid. Liquid growth medium is thus in contact with the pollen grain and the distal part of the tube, but the tip grows in air.

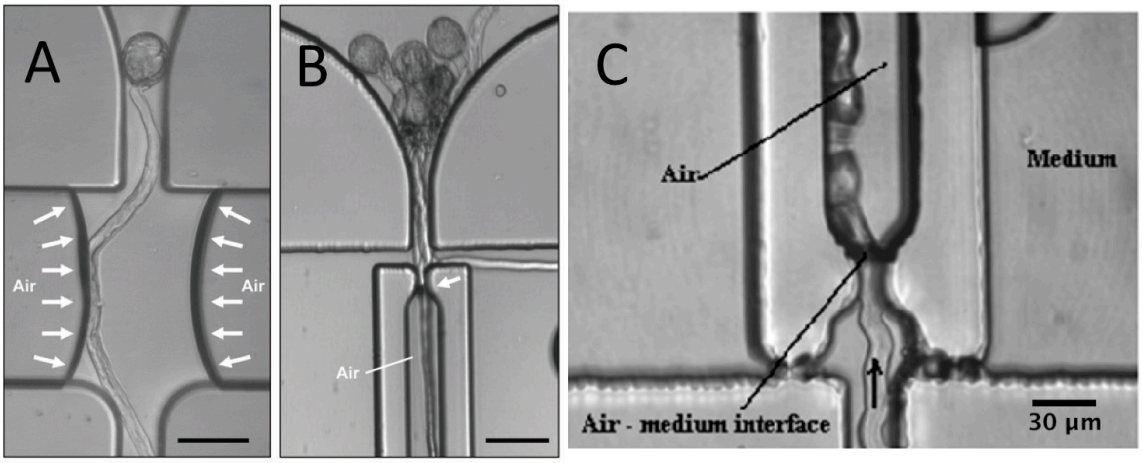

Figure 19. Growth of *Camellia* pollen tube in air chamber of the TipChip. (A) Pollen tubes normally avoid the air bubbles trapped inside the TipChip, microfluidic network. The arrows indicate the border of liquid medium and air. Scale bar = 100 µm. (B) An air chamber device with two horizontal microcantilevers that permit the pollen tubes to pass through the gap into the air chamber. The arrow represents the air-liquid interface. Scale bar = 100 µm. (C) Close-up of image B, growth of pollen tube inside air space. Scale bar = 30 µm.

Camellia pollen tubes penetrated inside the air chamber and elongated up to 1 mm in air (n = 19). We assume water vapour is the only source of water available to the growing tip in the air chamber. Thus, unless the pollen tube can utilize water vapour, its only source of water is that entering the pollen grain or the distal part of tube, which are immersed in growth medium. Similarly, nutrients and ions must be obtained from the grain or distal part of the tube, or they move from there through the cell wall to enter the cell near the apex. In the latter scenario, to sustain a standard growth rate of 14 µm min^{-1}, a flow speed of almost 300 µm min^{-1} through the cell wall would be required (Agudelo *et al*., 2013).

The scenario in which water is absorbed through the distal region of pollen tube raises questions both about the cell wall composition in that portion of the cell since it had been assumed to be rather impermeable (Geitmann and Steer, 2006) and the plasma membrane composition (Hill *et al*., 2012). Also, since calcium was thought to enter the tube only from the tip, the growth of pollen tube in air is difficult to reconcile with existing paradigms (Feijó *et al*., 2001; Hepler, 2005). Therefore, additional investigations are required to explain our findings. The air space design could also be used for the application of pharmacological agents on only the distal part of the pollen tube.

6.2. Directional memory

Some types of tip growing cells have a memory that allows them to reorient into their original growth direction once a mechanical obstacle is circumvented. This has been shown for the root hairs of *Dionaea muscipula* (Baluska, 2009). It is unknown whether pollen tubes have such a memory and given the difference in biological function between pollen tubes and root hairs, this question is worthwhile investigating. To do so, we designed an LOC with

microchannels (Figure 21) that force pollen tubes to change their growth direction several times before offering them a large cavity where their growth is not mechanically confined. Different shapes of microchannels were designed for this purpose, ranging from curved, zigzag and 90° angles.

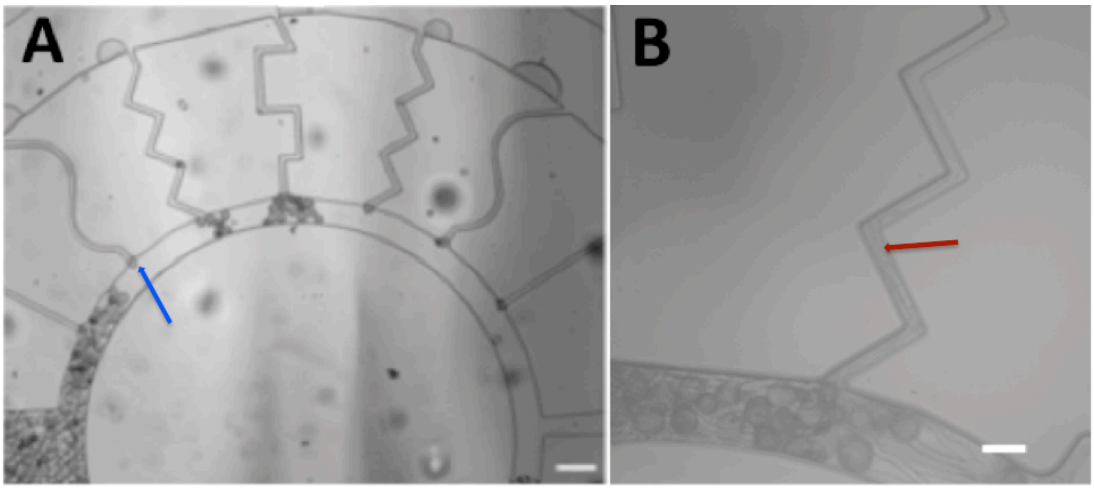

Figure 20. Presentation of the LOC for tip memory of pollen tube. (A) TipChip device for reorientation and directional memory shows the entrance of pollen tube (blue arrow) and the wide chamber at the end of the microchannel (B) Pollen tube growing inside the zigzag microchannel (red arrow). Scale bars= 50μm.

A sinusoidal shape of the microchannel (Figure 22 A and B) caused the pollen tube to always grow straight as long as possible until it was bent by the oblique angle of the wall. In microchannels with sharper turns, the pollen tube kept its direction until it hit a wall, typically stalled for a while, and then continued growing in a new direction permitted by the channel geometry (Figure 22 C, n = 20).

A pollen tube entering the wider chamber after repeated changes in direction (Figure 22A and B, indicated by arrow) continued growing in the direction it had when exiting the

microchannel rather than reorienting to its initial direction (n = 10). This contrasted with the reorientation behavior that was reported for root hairs (Bibikova *et al*., 1997) and fungal hyphae (Held *et al*., 2011). The absence or presence of a directional memory probably depends on the biological needs of the specific cell. Growing root hairs have the purpose to grow away from the roots to provide the plant with nutrients and water. Therefore, returning to the original growth direction after passing an obstacle optimizes this behavior. A fungal hypha also reorients after changing direction (for water and nutrients from either a biotic host or abiotic substrate) when it meets an obstacle. In contrast, a pollen tube has to follow the guidance cues of the pistil and female gametophyte, and the relative position of the pollen grain is irrelevant.

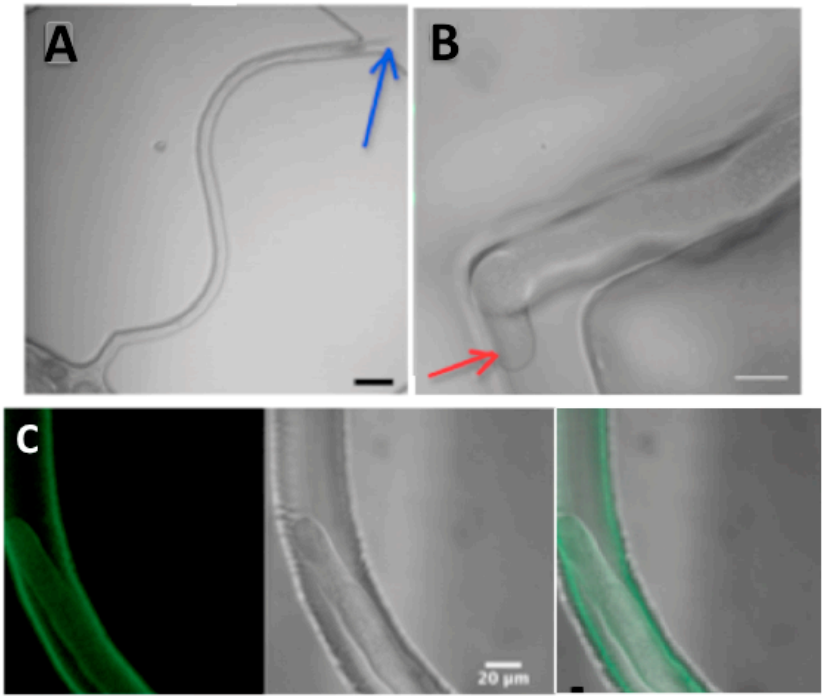

Figure 21. Growth of *Camellia* pollen tube inside LOC device designed to test directional memory. (A) Pollen tube entering wide chamber after passage through microchannel does not reorient to the original growth direction (blue arrow), (B) A reoriented pollen tube after encountering a 90° angle (red arrow), (C) Growth of pollen tube inside sinusoidal microchannel. Here vesicles were labelled with FM1-43 dye. The micrographs show the fluorescence, DIC and overlay. Scale bars= (A) 50 µm, (B) 30 µm, (C) 20 µm.

7. General Discussion & Perspectives

Fungal hyphae, root hairs or pollen tubes are tip-growing cells, which similar to neurons, invade their surrounding area, where they elongate to reach target. The stiff wall at the exterior of the membrane in plant and fungal cells makes their growth and elongation different from the non-walled cells. Understanding how these cells regulate the cell wall mechanical properties to control growth is therefore fundamental to our understanding of cellular functioning.. The growth path affects the mechanical properties of these walled cells. To imitate *in vivo* growth conditions the *in vitro* system has to simulate the *in vivo* biomechanical aspects. The growth process in pollen tubes is located at the apex of the cell. Since pollen tube elongates through the pistil, it has to penetrate, invade and reorient to reach an ovule for fertilization. Although the chemotropic behavior of the pollen tube in response to the chemical signals emitted from the female tissues has been studied, the mechanical behaviour of pollen tube is not well understood. Therefore, we successfully designed a novel device based on lab-on-chip (LOC) technology to create *in vitro* conditions that mimic certain aspects of the *in vivo* environment. This device allowed us to measure the invasion force and growth direction parameters of the pollen tube during growth and elongation. Our model system is the pollen tube of *Camellia japonica* in this study. Our results revealed changes in growth velocity, when pollen tube passed through narrow spaces during penetration. On its path through the differently sized gaps, the pollen tube either pushed the elastic PDMS sidewalls or decreased its width diameter to pass through the narrow spaces. Some pollen tubes stalled in the gap for several minutes. The pollen tube burst either inside or just after exiting the gap, mostly passing through the 3rd and 4th gaps, which were 13 or 11 μm wide, respectively. The time required to pass the micro-gap was inversely correlated with its width suggesting that narrower gaps (spaces) reduce the growth rate of pollen tube.

In addition, we found that the pollen tube dose not have any directional memory as is the case for root hairs and fungal hyphae. Pollen tube also showed the ability to grow in air, in the

absence of growth medium in the growing tip region of the tube. Since cell wall mechanics regulates pollen tube growth rate and morphology, and turgor pressure drives cell expansion and provides the invasion force (Winship *et al*. 2010, 2011), the ability of the pollen tube to grow in air encouraged us to further study the effects of osmotic medium on the growth behaviour at the tip when growth medium is only supplied to the distal portion of the pollen tube. Modulating the osmotic pressure in the medium can affect the pollen tube growth behaviour (Zerzour *et al*., 2009; Chebli and Geitmann, 2007) and, it would be interesting to investigate how a modulation in the turgor pressure affects the pollen tube's invasive force and its capacity to pass the narrow gaps. Further studies will therefore focus on the role of the osmotic value of medium and turgor pressure in invasion and penetration, and the role of the actin cytoskeleton and vesicle trafficking on directional growth.

Invasion of narrow spaces

The invasion capacity of pollen tube is based on both the ability of the tube to exert a force and its flexibility for entering narrow spaces. How each of these influence invasion was one of the purposes of this study. To better understand the invasive growth of the pollen tube, we developed an experimental setup to expose the elongating pollen tubes to elastic but mechanically impeding mechanical obstacles (Figure 12 and 14). The relative short length of the gaps allowed us to also study the recovery of pollen tubes after gap passage. Depending on the relative size of the tube compared to the gap, the pollen tube behaved differently. Those tubes that narrowed during the gap or widened after passing the gap, returned to their previous size quite rapidly after passing the obstacle. This observation indicates that internal processes govern the shape of the cell and thus ensure that the male germ unit can be transferred through the tube without getting stuck. Theoretical modeling has been done to explain how the diameter of pollen tube is determined (Fayant *et al*., 2010; Kroeger and Geitmann, 2012), but how this

mechanism operates biologically is not completely understood.

Pollen tube bursting after the gap passage opened the way for questions to be posed regarding the mechanism of sperm cell release *in vivo*. According to our experiments, a narrow opening is able to act as a trigger pollen tube discharge, which they could be either the ovule surface (teguments), the layers around the female gametophyte, or the filiform apparatus of synergids (Figure 5). However, the bursting only occured within a size ratio range of 1.20 and 1.33. Therefore, depending on the both pollen tube diameter and on the size of the gap, only correspondingly sized pollen tubes would be triggered to burst. Whether this mechanism is therefore biologically relevant is unkown.. Proteic and other chemical signals therefore need to be investigated further (Berger *et al*., 2008; Amien *et al*., 2010).

The interest for studying invasive growth has encouraged researchers to design ingenious methods ranging from gold foil as substrate (Miyoshi, 1985) to an optical waveguide (Bechinger *et al*., 1999), strain gauge (Money, 2001), and optical tweezers and beads (Wright *et al*., 2005). The technique of Lab-On-Chip and MEMS (microelectro-mechanical systems) technology that we used enabled us to produce a micro-structural environment mimicking the cells face in vivo (Sanati Nezhad *et al*., 2013a). The success of these techniques stems from the combination of experimentation and computation. Finite element modelling allowed us to calculate the forces involved in the passage of the tip-growing cell through an obstacle (Sanati Nezhad *et al*., 2013a). Using the MEMS-based devices we will in the future be able to control the cellular parameters such as turgor pressure and the mechanical properties of the cell wall and their interaction. Knowing these parameters is necessary for the understanding of the invasive force generation by tip-growing cells (Sanati Nezhad *et al*., 2013a). We hope that both technical and computational advances will enable us to quantify other forces as well, such as friction between the advancing cell and the substrate.

Studying invasive growth and cellular behaviour in natural growth conditions is one the

challenges associated with this subject. The LOC technique we developed allowed us to gain some sort of understanding of how the tube grows when it has to navigate a substrate or when it encounters obstacles. However, imaging of the true *in vivo* situation is eventually required and will necessitate imaging techniques able to penetrate deeper into the tissues than conventional confocal laser scanning microscopy.

Multi-photon excitation microscopy is one of the techniques that has been employed successfully for deep tissue imaging. In this technique the localized non-linear excitation applies for the excitation of fluorescence within a thin raster-scanned plane. Because the absorption is exactly on the focused area of the specimen and since red light is used that can penetrate deeper into the tissue, processes covered by overlaying tissues can be imaged. This technique was used to monitor nerve development in brain slices and living animals (Svoboda *et al*., 1996), growth of pollen tubes inside the pistillar tissue (Cheung *et al*., 2010), and invasion of tissue by tumor cells (Gatesman Ammer *et al*., 2011). There are other deep imaging techniques such as light sheet microscopy those have essential role in the advanced *in situ* observation approaches.

During growth, there is relationship between turgor pressure, up taking water and cell wall mechanic those build the dynamic force for tube elongation (Geitmann and Steer, 2006; Fayant *et al*., 2010; Rojas *et al*., 2011). In elongating lily pollen tube vesicles deliver the cell wall material to the apical region at tip of pollen tube (Bove *et al*., 2008). At the very small region of tip, this turgor pressure expands the cell wall of tip growing cells (Chebli and Geitmann, 2007; Fayant *et al.,* 2010). Since it was thought that changes in cell wall conditions could regulate the invasive force in tip-growing cells, our investigation of passing *Camellia* pollen tube through a gap could strongly verify this theory.

Additionally, the ability of LOC devices to be mounted on microscopes, even on laser scanning confocal microscope, enables us and other researchers to study intracellular processes

such as the motion of fluorescently labelled organelles or macromolecules.

We were able to demonstrate the usefulness of our innovative LOC *in vitro* system for the investitation of the biomechanical behaviour of pollen tubes and believe that this approach may be useful for other tip-growing cells as well.

Finally, invasive growth can only be completely understood when the other close-related processes like the mechanisms controlling growth direction are considered. In many tip-growing cell types, chemical and mechanical guidance (from either an appropriate target or the invaded substrate) determines invasive growth behavior (Palanivelu and Preuss, 2000; Chebli and Geitmann, 2007). What and how the mechanical limitation of invasive growth integrates with the directional mechanism opens questions for future experiments and modelling strategies.

References

- Agudelo, C., Packirisamy, M., and Geitmann, A. (2014). Lab-on-a-Chip for studying growing pollen tubes. *Plant Cell Morphogenesis: Methods and Protocols, Methods in Molecular Biology, 1080: 237-248*.

- Agudelo, C.G., Sanati Nezhad, A., Ghanbari, M., Naghavi, M., Packirisamy, M., and Geitmann, A. (2013). TipChip - a modular, MEMS (microelectromechanical systems)-based platform for experimentation and phenotyping of tip growing cells. *The Plant Journal, 73:1057-1068*.

- Agudelo, C., Sanati Nezhad, A., Ghanbari, M., Packirisamy, M. and Geitmann, A. (2012) A microfluidic platform for the investigation of elongation growth in pollen tubes. *Journal of Micromechanical Microengineering, 22, 115009: 1-11*.

- Alessa, L., and Kropf, D.L. (1999). F-actin marks the rhizoid pole in living *Pelvetia* compressa zygotes. *Development, 126:201-209*.

-Amien, S., Kliwer, I., Márton, M.L., Debener, T., Geiger, D., Becker, D., and Dresselhaus, T. (2010). Defensin-like ZmES4 mediates pollen tube burst in maize via opening of the potassium channel KZM1. *PLoS Biology, 8:1-13*.

-Armani, D., Liu, C., and Aluru, N. (1999). Re-configurable fluid circuits by PDMS elastomer micromachining. *IEEE Journal, 222-227*.

- Åström, H., Sorri, O., and Raudaskoski, M. (1995). Role of microtubules in the movement of the vegetative nucleus and generative cell in tobacco pollen tubes. *Sexual Plant Reproduction 8:61-69*.

- Baluška, F., and Mancuso, S. (2009). Plant neurobiology - From stimulus perception to adaptive behavior of plants, via integrated chemical and electrical signaling. *Plant Signal Behavior 4: 475–476.*

- Baluška, F., Salaj, J., Mathur, J., Braun, M., Jasper, F., Samaj, J., Chua, N.H., Barlow, P.W.,

and Volkmann, D. (2000). Root hair formation: F-actin dependent tip growth is initiated by local assembly of profilin supported F-actin meshworks accumulated within expansin enriched bulges. *Developmental Biology, 227: 618-632*.

- Bechinger, C., Giebel, K. F., Schnell, M., Leiderer, P., Deising, H. B. and Bastmeyer, M. (1999). Optical measurements of invasive forces exerted by appressoria of a plant pathogenic fungus. *Science 285: 1896-1899*.

- Beer, F.P., and Johnston, Jr, E.R. (1974). Mechanics of Materials. McGraw-Hill, New York. 832 pages.

- Benkert, R., Obermeyer, G., Bentrup, F.W. (1997). The turgor pressure of growing lily pollen tubes. *Protoplasma 198, 1:1-8*.

- Berger, F., Hamamura, Y., Ingouff, M., and Higashiyama, T. (2008). Double fertilization - caught in the act. *Trends in Plant Science 13:437-443*.

- Bibikova, T.N., Zhigilei, A., and Gilroy, S. (1997). Root hair growth in *Arabidopsis thaliana* is directed by calcium and an endogenous polarity. *Planta 203: 495–505*.

- Bove, J., Vaillancourt, B., Kroeger, J., Hepler, P. K., Wiseman, P. W., and Geitmann, A. (2008). Magnitude and direction of vesicle dynamics in growing pollen tubes using spatiotemporal image correlation spectroscopy and fluorescence recovery after photobleaching. *Plant Physiology 147:1646-1658*.

- Bou Daher, F. (2011). Actin cytoskeleton regulates pollen tube growth and tropism. PhD thesis, University of Montreal.

- Bou Daher, F., and Geitmann, A. (2011). Actin regulates pollen tube tropism through redirection of secretory vesicles. *Traffic, 12: 1537–1551*.

- Bou Daher, F., and Geitmann, A. (2011). Spatial and temporal expression of actin depolymerizing factors ADF7 and ADF10 during male gametophyte development in *Arabidopsis thaliana*. *Plant Cell Physiology 52: 1177–1192*.

- Bubendorfer, A., Liu, X., and Ellis, A. (2007). Microfabrication of PDMS microchannels using SU-8/PMMA moldings and their sealing to polystyrene substrates. *Smart Material Structure, 16: 367–371*.

- Castle, E. S. (1955). The mode of growth of epidermal cells of the *Avena coleoptile*. *Proceeding of National Academy of Sciences of USA, 41: 197-199*.

- Chantha, S-C., Tebbji, F, and Matton, D. P. (2007). From the Notch Signaling Pathway to Ribosome Biogenesis. *Plant Signaling & Behavior 2: 168-170*.

- Chebli, Y., & Geitmann, A. (2007). Mechanical principles governing pollen tube growth. *Functional Plant Science and Biotechnology*, *1: 232-245*.

- Chen, C. Y., Wong, E. I., Vidali, L., Estavillo, A., Hepler, P. K. , Wu, H.M., and Cheung, A. Y. (2002). The regulation of actin organization by actin depolymerizing factor in elongating pollen tubes. *Plant Cell 14: 2175-2190*.

- Chen, J.C.W. (1973). The kinetics of tip growth in the *Nitella* rhizoid. *Plant Cell Physiology 14: 631-640*.

- Cheung, A.Y., and Wu, H.M. (2008). Structural and signaling networks for the polar cell growth machinery in pollen tubes. *Annual Review of Plant Biology, 59: 547-572*.

- Cojoc, D., Difato, F., Ferrari, E., Shahapure, R.B., Laishram, J., Righi, M., Di Fabrizio, E.M., and Torre, V. (2007). Properties of the force exerted by filopodia and lamellipodia and the involvement of cytoskeletal components. *PLoS One, 2: 1-8*.

- Cosgrove, D.J. (2005). Growth of the plant cell wall. *Nature Review Molecular Cell Biology, 6: 850–861*.

- Cosgrove, D. J. (2000). Expansive growth of plant cell walls. *Plant Physiology and Biochemistry, 38: 109−124*.

- Dent, E.W., Gertler, F.B. (2003). Cytoskeletal dynamics and transport in growth cone motility and axon guidance. *Neuron 40: 209–227*.

- Dickson, B.J. (2002). Molecular Mecahniasm of Axon Guidance. *Scince, 298: 1959-1964*.

- Dumais, A., Shaw, S. L., Steele, C. R., Long, S. R., and Ray, P. M. (2006). An anisotropic-viscoplastic model of plant cell morphogenesis by tip growth. *International Journal of Developmental Biology, 50: 209-222*.

- Drubin, D.G., and Nelson, W.J. (1996). Origins of cell polarity. *Cell, 84: 335-344*.

- Erbar C. (2003). Pollen tube transmitting tissue: Role of comptetition of male gametophytes. *International Journal of Plant Science 164:S265-S277.*

- Fayant, P., Girlanda, O., Chebli, Y., Aubin, C.E., Villemure, I., and Geitmann, A. (2010). Finite element model of polar growth in pollen tubes. *Plant Cell Reports, 22:2579-2593*.

- Felle, H. H., Herrmann, A., Hückelhoven, R., and Kogel, K.-H. (2005). Root-to-shoot signalling: apoplastic alkalinization, a general stress response and defence factor in barley (*Hordeum vulgare*). *Protoplasma, 227: 17–24*.

- Feijó, J.A., Sainhas, J., Holdaway-Clarke, T.L., Cordeiro, M.S., Kunkel, J.G. and Hepler, P.K. (2001). Cellular oscillations and the regulation of growth: the pollen tube paradigm. *BioEssays, 23: 86–94*.

- Friese, M. E. J., Nieminen, T. A., Heckenberg, N. R., and Rubinsztein-Dunlop, H. (1998). Optical alignment and spinning of laser-trapped microscopic particles. *Nature 394, 348-350*.

- Ferguson, C., Teeri, T.T., Siika-aho, M., Read, S.M., Bacic, A. (1998). Location of cellulose and callose in pollen tubes and grains of *Nicotiana tabacum*. *Planta (1998) 206: 452-460*.

- Fowler, J. E., and Quatrano, R. S. (1997). Plant cell morphogenesis: plasma membrane interactions with the cytoskeleton and cell wall. *Annual Review of Cell Development and Biology, 13:697–743*.

- Fuard, D., Tzvetkova-Chevolleau, T., Decossas, S., Tracqui, P., and Schiavone, P. (2008). Optimization of poly-di-methyl-siloxane (PDMS) substrates for studying cellular adhesion and motility. *Microelectronic Engineering, 85:1289–1293*.

- Gasser, C.S., and Robinson-Beers, K. (1993) Pistil development. *Plant Cell 5:1231-1239*.

- Gatesman Ammer, A., Hayes, K., Martin, K., Zhang, L., Spirou, G., and Weed, S. (2011). Multi-photon imaging of tumour cell invasion in an orthotopic mouse model of oral squamous cell carcinoma. *Journal of Visualized Experiments, 53: 2941.*

- Gebert, M., Dresselhaus, T., and Sprunck, S. (2008). F-Actin organization and pollen tube tip growth in *Arabidopsis* are dependent on the gametophyte-specific armadillo repeat protein ARO1. *The Plant Cell, 20: 2798–2814*.

- Geitmann, A. and Palanivelu, R. (2007). Fertilization requires communication: signal generation and perception during pollen tube guidance. *Floriculture and Ornamental Biotechnology 1: 77-89*.

- Geitmann, A., and Steer, M. (2006). The architecture and properties of the pollen tube cell wall, In R. Malhó, The Pollen Tube, Plant Cell Monograph (3), Springer-Verlag Berlin Heidelberg, pp.177-200.

- Geitmann, A., Snowman, B.N., Emons, A.M.C., and Franklin-Tong, V.E. (2000). Alterations in the actin cytoskeleton of pollen tubes are induced by the self-incompatibility reaction in *Papaver rhoeas*. *Plant Cell 12: 1239–1251*.

- Gossot, O., and Geitmann, A. (2007). Pollen tube growth: coping with mechanical obstacles involves the cytoskeleton. *Planta, 226: 405-416*.

- Gönczy, P., and Hyman, A.A. (1996). Cortical domains and the mechanisms of asymmetric cell division. *Trends in Cell Biology. 6: 382–87.*

- Greaves, G.N., Greer, A.L., Lakes, R.S., and Rouxe, T. (2011). Poisson's ratio and modern materials. *Nature Materials. 10: 823-837*

- Green, P.B. (1963). Cell walls and the geometry of plant growth. In Meristems and Differentiation. *Brookhaven Symposia in Biology 16: 203-217*.

- Gu ,Y., Vernoud, V., Fu, Y., and Yang, Z. (2003). ROP GTPase regulation of pollen tube growth through the dynamics of tip-localized F-actin. *Journal of Experimental Botany, 54:93-101*.

- Hable, W.E., Miller, N.R., and Kropf, D.L. (2003). Polarity establishment requires dynamic actin in fucoid zygotes. *Protoplasma, 221:193-204*.

- Haling, R. E., Brown, L. K., Bengough, A. G., Young, I. M., Hallett, P. D., White, P. J., and George, T. S. (2013). Root hairs improve root penetration, root–soil contact, and phosphorus acquisition in soils of different strength. *Journal of Experimental Botany, 64: 3711–3721*.

- Hamant, O., Heisler, M.G., Jönsson, H., Krupinski, P., Uyttewaal, M., Bokov, P., Corson, F., Sahlin, P., Boudaoud, A., Meyerowitz, E.M., Couder, Y., Traas, J. (2008) Developmental patterning by mechanical signals in *Arabidopsis*. *Science 322, 1650–1655*.

- Harris, S. D. (2008). Branching of fungal hyphae: regulation, mechanisms and comparison with other branching systems. *Mycologia, 100: 823–832*.

polarity and guidance by nerve growth factor. *Journal of Neurobiology 66: 847–867*.

- Haydon, P. (1988). The formation of chemical synapses between cellcultured neuronal somata. *Journal of Neuroscience 8: 1032–1038*.

- Hedrich, R., Neimanis, S., Savchenko, G., Felle, H. H., Kaiser, W. M., and Heber, U. (2001). Changes in apoplastic pH and membrane potential in leaves in relation to stomatal responses to CO_2, malate, abscisic acid or interruption of water supply. *Planta, 213, 4: 594-601*.

- Held, M., Edwards, C., and Nicolau, D. (2011). Probing the growth dynamics of *Neurospora crassa* with microfluidic structures. *Fungal Biology, 115: 493–505*.

- Hepler PK, Vidali L, and Cheung AY: Polarized cell growth in higher plants. *Annual Review*

of Cell Development Biology, 17:159-187.

- Higashiyama, T., and Hamamura, Y. (2008). Gametophytic pollen tube guidance. *Sextual Plant Reproduction, 21:17–26*.

- Horvitz, H.R., and Herskowitz, I. (1992). Mechanisms of asymmetric cell division: two Bs or not two Bs that is the question. *Cell 68:237–55*.

- Howard RJ, Valent B (1996) Breaking and entering: host penetration by the fungal rice blast pathogen *Magnaporthe grisea*. *Annual Reviews in Microbiology 50, 1:491-512*.

- Hülskamp, M., Schneitz, K., and Pruitt, R. E. (1995). Genetic evidence for a long-range activity that directs pollen tube guidance in *Arabidopsis*. *Plant Cell 7:57-64*.

- Inoué, S. and Sato, H. (1976). Cell motility by labile association of molecules; The nature of mitotic spindle fibers and their role in chromosome movement. *Journal of General Physiology, 50, 6: 259-292*.

- Isbister, C. M. and O'Connor, T. P. (2000). Mechanisms of growth cone guidance and motility in the developing grasshopper embryo. *Journal of Neurobiology 44:271-280*.

- Ishijima, A., Doi, T., Sakurada, K., Yanagida, T. (1991). Subpiconewton force fluctuations of actomyosin *in vitro*. *Nature 352:301-306*.

- Johnson-Brousseau, S. A. and S. McCormick (2004). A compendium of methods useful for characterizing Arabidopsis pollen mutants and gametophytically expressed genes. *Plant Journal 39: 761-775.*

- Keegstra, K. (2010). Plant cell walls. *Plant Physiology, 154: 483–486.*

- Kidambi, S., Udpa, N., Schrosder, S.A., Findlan, R., Lee, I., and Chen, C. (2007). Cell adhesion on polyelectrolyte multilayer coated polydimethylsiloxane surfaces with varying topographies. *Tissue Engineering, 13:2105-2117*.

- Kobel, S., Valero, A., Latt, J., Renaud, P., and Lutolf, M. (2010). Optimization of microfluidic single cell trapping for long-term on-chip culture. *Lab Chip, 10, 857–863*.

- Kovar, D. R., Drobak, B. K., and Staiger, C. J. (2000). Maize profiling isoforms are functionally distinct. *Plant Cell 12: 583-598*.

- Krichevsky, A., Kozlovsky, S.V., Tian, G.W., Chen, M.H., Zaltsman, A., and Citovsky, V. (2007). How pollen tubes grow. *Developmental Biology 303, 2: 405-420.*

- Kroeger, J., and Geitmann, A. (2012). Pollen tube growth: getting a grip on cell biology through modeling. *Mechanics Research Communications 42:32-39*.

- Kropf, D.L. (1992). Establishment and expression of cellular polarity in fucoid zygotes. *Microbiological Review, 56:316–39*.

- Kumar S, Weaver VM. 2009. Mechanics, malignancy, and metastasis: the force journey of a tumor cell. *Cancer and Metastasis Reviews 28, 113–127*.

- Lennon, K.A., Roy, S., Hepler, P.K., and Lord, E.M. (1998). The structure of the transmitting tissue of *Arabidopsis thaliana* (L.) and the path of pollen tube growth. *Sexual Plant Reproduction, 11:49-59*.

- Lew R.R. (2005) Mass flow and pressure-driven hyphal extension in *Neurospora crassa*. *Microbiology, 151:2685-2692*.

- Liu, G. (2003). Meshfree Methods: Moving Beyond the Finite Element Method. (CRC Press), Science.

- Lord, E. M., and Russell, S. D. (2002). The mechanisms of pollination and fertilization in plants. *Annual Review of Cell Developmental Biology, 18:81–105.*

- Loudon, R.P., Silver, L.D., Yee, H.F. Jr., Gallo, G. (2006). RhoA-kinase and myosin II are required for the maintenance of growth cone polarity and guidance by nerve growth factor. *Journal of Neurobiology, 66:847-867*.

- Major, G., Daigle, C., Stafford-Richard, T., Tebbji, F., Lafleur, É., Caron, S., and Matton, D.P. (2009). Characterization of *ScMAP4K1*, a MAP kinase kinase kinase kinase involved in ovule,

seed and fruit development in *Solanum chacoense* Bitt. *Current Topics in Plant Biology*, *10: 27-46*.

- Mathur, J. (2006). Local interactions shape plant cells. *Current Opinion in Cell Biology, 18:40–46*.

- Mathur J. (2004). Cell shape development in plants. *Trends in Plant Science, 9:583-590*.

- Mathur, J., Spielhofer, P., Kost, B., and Chua, N. (1999). The actin cytoskeleton is required to elaborate and maintain spatial patterning during trichome cell morphogenesis in *Arabidopsis thaliana. Development, 126: 5559-5568*.

- Mattila, P.K., and Lappalainen, P. (2008). Filopodia: molecular architecture and cellular functions. *Nature 9: 446-454*.

- Miyoshi, M. (1895). Die Durchbohrung von Membranen durch Pilzfäden. Jahrbücher der Wissenschaft in Botanik. 28: 269-289.

- Money, N.P. (1997). Wishful thinking of turgor revisited: The mechanics of fungal growth. *Fungal Genetics and Biology, 21:173- 187*.

- Money, N.P. (2004). The fungal dining habit: a biomechanical perspective. *Mycologiste 18*: *71-76*.

- Money, N.P., Davis, C.M., and Ravishankar, J.P. (2004). Biomechanical evidence for convergent evolution of the invasive growth process among fungi and oomycete water molds. *Fungal Genetics and Biology 41:872-876*.

- Money, N.P. (2007). Biomechanics of invasive hyphal growth. *Biology of the Fungal Cell*, eds Howard R.J., Gow N.A.R. (Springer, Berlin), pp 237–249.

- O`Brien, S., (1994). Pistil structure and pollen tube pathway in *Leptospermum myrsinoides* and *L. Continentale* (Myrtaceae). *Annals of Botany, 73: 225-230*.

- Palanivelu, R., and Preuss, D. (2000). Pollen tube targeting and axon guidance: parallels in tip growth mechanisms. *Trends in Cell Biology, 10: 517-524*.

- Park, A-Y., Jauh, G-Y., Mollet, J-C., Eckard, K. J., Nothnagel., E. A., Walling, L. L., and Lord, E. M. (2000). A Lipid Transfer–like Protein Is Necessary for Lily Pollen Tube Adhesion to an in Vitro Stylar Matrix. *The Plant Cell, 12: 151–163*.

- Park, J.H., Park, K.D., and Bae, Y.H. (1999). PDMS-based polyurethanes with MPEG grafts: synthesis, characterization and platelet adhesion study. *Biomaterials, 20: 943-953*.

- Parre, E. and Geitmann, A. (2005) More than a leak sealant – the physical properties of callose in pollen tubes. *Plant Physiology, 137: 274–286*.

- Pei, W., Du, F., Zhang, Y., He, T., and Ren, H. (2012). Control of the actin cytoskeleton in root hair development. *Plant Sceince, 187: 10-18*.

- Pierson, E.S., Derksen, J., and Traas, J.A. (1986). Organization of microfilaments and microtubules in pollen tubes grown in vitro or in vivo in various angiosperms. *European Journal of Cell Biology, 41: 14–18*.

- Qin, Y., Wysocki, R.J., Somogyi, A., Feinstein, Y., Franco, J.Y., Tsukamoto, T., Dunatunga, D., Levy, C., Smith, S., Simpson, R., Gang, D., Johnson, M.A., Palanivelu, R. (2011). Sulfinylated azadecalins act as functional mimics of a pollen germination stimulant in *Arabidopsis* pistils. *The Plant Journal, 68: 800-815*.

- Raghavan, V. (1997) Molecular Embryology of Flowering Plants. *Cambridge University Press, Cambridge, UK ; pp. 690*.

- Rojas, E., Hotton, S., and Dumais, J. (2011). Chemically mediated mechanical expansion of the pollen tube cell wall. *Biophysical Journal 101:1844–1853*.

- Roy, S.J., Holdaway-Clarke, T.L., Hackett, G.R., Kunkel, J.G., Lord, E.M. and Hepler, P.K. (1999) Uncoupling secretion and tip growth in lily pollen tubes: evidence for the role of calcium in exocytosis. *Plant Journal, 19: 379-386*.

- Sanati Nezhad, A., Naghavi, M., Packirisamy, M., Bhat, R., Geitmann, A. (2013a).

Quantification of cellular penetrative forces using Lab-on-a-Chip technology and finite element modeling. *Proceedings of the National Academy of Sciences of the United States of America*, *110: 8093-8098.*

- Sanati Nezhad, A., Naghavi, M., Packirisamy, M., Bhat, R., Geitmann, A. (2013b). Quantification of the Young's modulus of the primary plant cell wall using Bending-Lab-On-Chip (BLOC). *The Royal Society of Chemistry (RSC) Journal, 13: 2599-2608*.

- Sanati Nezhad, A., Packirisamy, M., Bhat, R., Geitmann, A. (2013c). In vitro study of oscillatory growth dynamics of *Camellia* pollen tubes in microfluidic environment. *IEEE Transactions on Biomedical Engineering*, *60: 3185-3193.*

- Sanati Nezhad, A., Ghanbari, M., Agudelo, C.G., Naghavi, M., Packirisamy, M., Bhat, R.B., and Geitmann, A. (2013d). Optimization of flow assisted entrapment of pollen grains in a microfluidic platform for tip growth analysis. *Biomedical Microdevices*, *13: 9802-9808*.

- Sanati Nezhad, A., and Geitmann, A. (2013). The cellular mechanics of an invasive life style. *Journal of Experimental Botany, 64, 1-20*.

- Shaw, S.L., Dumais, J. and Long, S.R. (2000) Cell surface expansion in polarly growing root hairs of *Medicago truncatula*. *Plant Physiology, 124: 959-969*.

- Schopfer, P. (2006). Biomechanics of plant growth. *American Journal of Botany 93:1415-1425*.

- Smith, L.G., Oppenheimer, D.G. (2005). Spatial control of cell expansion by the plant cytoskeleton. *Annual Review of Cell and Developmental Biology 21:271-295*.

- Svoboda, k., Tank, D.W., and Denk, W. (1996). Direct measurement of coupling between dendritic spines and shafts. *Science, 272: 716-719*.

- Szymanski, D. B., and Cosgrove, D. J. (2009). Dynamic coordination of cytoskeletal and cell wall systems during plant cell morphogenesis. *Current Biology, 19: 800–811*.

- Takemoto, D., Tanaka, A., and Scott, B. (2006). A p67Phox-Like Regulator Is Recruited to

Control Hyphal Branching in a Fungal–Grass Mutualistic Symbiosis. *The Plant Cell, 18: 2807–2821*.

- Tan, W.H., and Takeuchi, S. (2007). A trap-and-release integrated microfluidic system for dynamic microarray applications. *Proceedings of the National Academy of Sciences of the USA, 104: 1146–1151*.

- Taylor, L. P., and Hepler, P. K. (1997). Pollen germination and tube growth. *Annual Review of Plant Physiology and Plant Molecular Biology, 48:461–91*.

- Theriot, J.A. (2000). The polymerization motor. *Traffic, 1:19-28*.

- Uwate, W.J., Lin, J., Ryugo, K., and Stallman, V. (1980). Cellular components of the midstylar transmitting tissue of *Prunus avium*. *Canadian Journal of Botany 60:98-104*.

- Veytsmann, B., and Cosgrove, D.J. (1998). A model of cell wall expansion based on thermodynamics of polymer networks. *Biophysical Journal, 75: 2240–2250*.

- Vidali, L., McKenna, S. T., and Hepler, P. K. (2001) Actin polymerization is essential for pollen tube growth. *Molecular Biology of the Cell*, *12: 2534–2545*.

- Vidali, L. and P. K. Hepler (1997). Characterization and localization of profilin in pollen grains and tubes of Lilium longiflorum. *Cell Motility and the Cytoskeleton 36: 323-338*.

- Wang, H., Wu, H-M., and Cheung, A. (1996). Pollination induces mRNA poly (A) tail-shortening and cell deterioration in flower transmitting tissue. *The Plant Journal 9:715-727*.

- Wiedemeier, A.M.D., Judy-March, J.E., Hocart. C.H., Wasteneys, G.O., Williamson, R.E., and Baskin, T.I. (2002). Mutant alleles of *Arabidopsis RADIALLY SWOLLEN 4* and *7* reduce growth anisotropy without altering the transverse orientation of cortical microtubules of cellulose microfibrils. *Development, 129: 4821–4830*.

- Williams, J. (2008). Novelties of the flowering plant pollen tube underlie diversification of a key life history stage. *Proceedings of the National Academy of Sciences of the United States of America, 105:11259–11263.*

- Winship, L.J., Obermeyer, G., Geitmann, A., and Hepler, P.K. (2010). Under pressure, cell walls set the pace. *Trends in Plant Science, 15: 363–369*.

- Winship, L.J., Obermeyer, G., Geitmann, A., and Hepler, P.K. (2011). Pollen tubes and the physical world. *Trends in Plant Science, 16: 353-355.*

- Wright, G., Arlt, J., Poon, W., and Read, N. (2005). Measuring fungal growth forces with optical tweezers. *Proceedings of SPIE 5930:F1–F7*.

- Yamaguchi H, Wyckoff J, Condeelis J. 2005. Cell migration in tumors. *Current Opinion in Cell Biology, 17, 559–564*.

- Yetisen, A. K., Jiang, L., Cooper, J. R., Qin, Y., Palanivelu, R., and Zohar, Y. (2011). A microsystem-based assay for studying pollen tube guidance in plant reproduction. *Journal of Micromechanics and Microengineering, 21: 1-9.*

- Yu, H., Meyvantsson, I., Shkel, I., and Beebe, D. (2005). Diffusion dependent cell behavior in microenvironments. *Lab Chip, 5: 1089–1095*.

- Zerzour, R., Kroeger, J., and Geitmann, A. (2009). Polar growth in pollen tubes is associated with spatially confined dynamic changes in cell mechanical properties. *Developmental Biology*, *334: 437-46*4.

- Zheng, J. Q., Wan, J. J., Poo, M. M. (1996). Essential role of filopodia in chemotropic turning of nerve growth cone induced by a glutamate gradient. *The Journal of Neuroscience, 16, 3: 1140-1149.*

- Zonia, L.E., Müller, M. and Munnik, T. (2006). Hydrodynamics and cell volume oscillations in the pollen tube apical region are integral components of the biomechanics of *Nicotiana tabacum* pollen tube growth. *Cell Biochem. Biophys, 46, 209–232*.

- Zwolinski, B. J., Eyring, H., and Reese, C. E. (1949). Diffusion and membrane permeability. *Journal of Physical Chemistry, 53: 1426–1453*.

Annex:

1- Agudelo, C.G., Sanati Nezhad, A., Ghanbari, M., Naghavi, M., Packirisamy, M., and Geitmann, A. (2013). TipChip - a modular, MEMS (microelectromechanical systems)-based platform for experimentation and phenotyping of tip growing cells. *The Plant Journal, 73:1057-1068*.

2- Sanati Nezhad, A., Naghavi, M., Packirisamy, M., Bhat, R., Geitmann, A. (2013). Quantification of the Young's modulus of the primary plant cell wall using Bending-Lab-On-Chip (BLOC). *The Royal Society of Chemistry (RSC) Journal, 13: 2599-2608*.